drugs and drug candidates

MDPI

Article

Design, Synthesis, and In Vitro Antimalarial Evaluation of New 1,3,5-*Tris*[(4-(Substituted-Aminomethyl)Phenoxy)Methyl]Benzenes

Sandra Albenque-Rubio [1], Jean Guillon [1,*], Patrice Agnamey [2], Céline Damiani [2], Solène Savrimoutou [1], Romain Mustière [2], Noël Pinaud [3], Stéphane Moreau [1], Jean-Louis Mergny [4], Luisa Ronga [5], Ioannis Kanavos [5], Mathieu Marchivie [6], Serge Moukha [7,8], Pascale Dozolme [7,8], Pascal Sonnet [2] and Anita Cohen [9]

1 Faculty of Pharmacy, University of Bordeaux, CNRS, INSERM, ARNA, UMR 5320, U1212, F-33076 Bordeaux, France; sandra.rubio@u-bordeaux.fr (S.A.-R.); solene.savrimoutou@u-bordeaux.fr (S.S.); stephane.moreau@u-bordeaux.fr (S.M.)
2 Faculty of Pharmacy, Agents Infectieux, Résistance et Chimiothérapie (AGIR), UR 4294, UFR de Pharmacie, University of Picardie Jules Verne, F-80037 Amiens, France; p.agnamey@u-picardie.fr (P.A.); damiani.celine@chu-amiens.fr (C.D.); romain.mustiere@u-picardie.fr (R.M.); pascal.sonnet@u-picardie.fr (P.S.)
3 ISM, CNRS, Bordeaux INP, UMR 5255, University of Bordeaux, F-33400 Talence, France; noel.pinaud@u-bordeaux.fr
4 Laboratoire d'Optique et Biosciences, Institut Polytechnique de Paris, Ecole Polytechnique, CNRS, INSERM, F-91120 Palaiseau, France; jean-louis.mergny@inserm.fr
5 Institut des Sciences Analytiques et de Physico-Chimie Pour l'Environnement et les Matériaux, Université de Pau et des Pays de l'Adour, E2S UPPA, CNRS, IPREM, F-64053 Pau, France; luisa.ronga@univ-pau.fr (L.R.); i.kanavos@univ-pau.fr (I.K.)
6 ICMCB—UMR 5026, University of Bordeaux, F-33608 Pessac, France; mathieu.marchivie@u-bordeaux.fr
7 Centre de Recherche Cardio-Thoracique de Bordeaux (CRCTB), UMR U1045 INSERM, PTIB—Hôpital Xavier Arnozan, F-33600 Pessac, France; serge.moukha@u-bordeaux.fr (S.M.); pascale.dozolme@u-bordeaux.fr (P.D.)
8 INRAE Bordeaux Aquitaine, F-33140 Villenave-d'Ornon, France
9 Faculty of Pharmacy, Aix-Marseille Université, MCT-UMR MD1, INSERM SSA U1261, F-13385 Marseille, France; anita.cohen@univ-amu.fr
* Correspondence: jean.guillon@u-bordeaux.fr; Tel.: +33-(0)5-57-57-16-52

Abstract: By taking into account our previously described series of 1,3,5-*tris*[(4-(substituted-aminomethyl)phenyl)methyl]benzene compounds, we have now designed, prepared, and evaluated in vitro against *Plasmodium falciparum* a novel series of structural analogues of these molecules, i.e., the 1,3,5-*tris*[(4-(substituted-aminomethyl)phenoxy)methyl]benzene derivatives. The pharmacological data showed antimalarial activity with IC_{50} values in the sub and μM range. The in vitro cytotoxicity of these new nitrogen polyphenoxymethylbenzene compounds was also evaluated on human HepG2 cells. The 1,3,5-*tris*[(4-(substituted-aminomethyl)phenoxy)methyl]benzene derivative **1m** was found as one of the most potent and promising antimalarial candidates with favorable cytotoxic to antiprotozoal properties in the *P. falciparum* strains W2 and 3D7. In conclusion, this 1,3,5-*tris*[(4-(pyridin-3-ylmethylaminomethyl)phenoxyl)methyl]benzene **1m** (IC_{50} = 0.07 μM on W2, 0.06 μM on 3D7, and 62.11 μM on HepG2) was identified as the most promising antimalarial derivative with selectivity indexes (SI) of 887.29 on the W2 *P. falciparum* chloroquine-resistant strain, and of 1035.17 on the chloroquine-sensitive and mefloquine decreased sensitivity strain 3D7. It has been previously described that the telomeres of *P. falciparum* could represent potential targets for these types of polyaromatic compounds; therefore, the capacity of our novel derivatives to stabilize the parasitic telomeric G-quadruplexes was assessed using a FRET melting assay. However, with regard to the stabilization of the protozoal G-quadruplex, we observed that the best substituted derivatives **1**, which exhibited some interesting stabilization profiles, were not the most active antimalarial compounds against the two *Plasmodium* strains. Thus, there were no correlations between their antimalarial activities and selectivities of their respective binding to G-quadruplexes.

check for updates

Citation: Albenque-Rubio, S.; Guillon, J.; Agnamey, P.; Damiani, C.; Savrimoutou, S.; Mustière, R.; Pinaud, N.; Moreau, S.; Mergny, J.-L.; Ronga, L.; et al. Design, Synthesis, and In Vitro Antimalarial Evaluation of New 1,3,5-*Tris*[(4-(Substituted-Aminomethyl) Phenoxy)Methyl]Benzenes. *Drugs Drug Candidates* **2024**, *3*, 615–637. https://doi.org/10.3390/ddc3030035

Academic Editor: Philippe Loiseau

Received: 11 July 2024
Revised: 6 September 2024
Accepted: 10 September 2024
Published: 13 September 2024

Keywords: antimalarial activity; 1,3,5-*tris*[(4-(substituted-aminomethyl)phenoxy)methyl]benzene; G-quadruplexes; synthesis

1. Introduction

According to the latest world malaria report, there were 249 million cases of malaria in 2022 compared to 244 million cases in 2021 [1]. The estimated number of malaria deaths in 85 countries stood at 608,000 in 2022 compared to 610,000 in 2021. The WHO African Region continues to carry a disproportionately high share of the global malaria burden. In 2022, Africa was home to about 94% of all malaria cases and 95% of deaths globally. Children under 5 years of age accounted for about 78% of all malaria deaths in these African countries [2], despite the WHO's recommendation to prevent malaria in children living in areas of risk, of the RTS,S/AS01 malaria vaccine in areas of moderate-to-high malaria transmission since October 2021 [3], and of the R21/Matrix-M (R21) vaccine in October 2023 [3].

Present challenges involve the infiltration of *Anopheles stephensi*, a mosquito capable of easily adapting to urban environments, which turns it into a highly competent vector of *P. falciparum* and *P. vivax*. Currently considered to be one of the most efficient vectors of malaria in urban environments, distinguishing it from other malaria vectors that breed mainly in rural areas, its spread in Africa, if left uncontrolled, combined with rapid and poorly planned urbanization, can increase the risk of malaria transmission, posing a significant threat to public health [4]. Additionally, issues such as resistance to pyrethroid insecticides and antimalarial drugs have become more pronounced. New innovations are being developed and recommended, such as the use of mosquito nets impregnated with a synergizer (piperonyl butoxide) or pro-insecticide (chlorfenapyr) in combination with a pyrethroid insecticide to which insects are increasingly resistant [1]. Thus, these difficulties have not only affected malaria control but have also impacted the management of other vector-borne neglected tropical diseases, such as leishmaniasis [5].

In response to these challenges, the WHO proposed a global strategy in the program titled "Ending the Neglect to Attain the Sustainable Development Goals: A Road Map for Neglected Tropical Diseases 2021–2030" [5]. This initiative, developed through a worldwide global consultation, underscores the fundamental role of "research and innovation as enablers of programmatic progress for all tropical diseases." Consequently, it appears crucial to integrate and enhance cross-cutting approaches, including the exploration of new treatment strategies and the investigation of community-based and applied research for various tropical diseases. Thus, one possibility would consist of the discovery of new treatments against malaria involving the design and synthesis of quinoline-based derivatives that evade recognition by the protein system responsible for drug efflux, as seen in the case of primaquine (PQ) or amodiaquine (AQ). Efflux pumps, which can function as both natural defense mechanisms and contributors to drug bioavailability and disposition, play a crucial role in this strategy. Initially observed in *Plasmodium falciparum*, where red blood cells infected with chloroquine (CQ)-resistant parasites accumulated less drug compared to sensitive ones, further analysis led to the identification of the *Pf*crt gene, among other mechanisms of quinoline compound resistance [6].

Previous studies have introduced novel series of compounds, such as bisquinoline A and bisacridine B antimalarial drugs (Figure 1, compounds A–B and Piperaquine), which have not been recognized by the protein system involved in drug efflux [6–13]. These newly developed compounds exhibit significantly lower resistance indices than chloroquine (CQ), indicating that these bis-heterocyclic derivatives are less efficiently rejected by the efflux mechanisms of drug-resistant parasites. More recently, tafenoquine, a new 8-aminoquinoline, was developed to prevent all types of malaria [10,12,14].

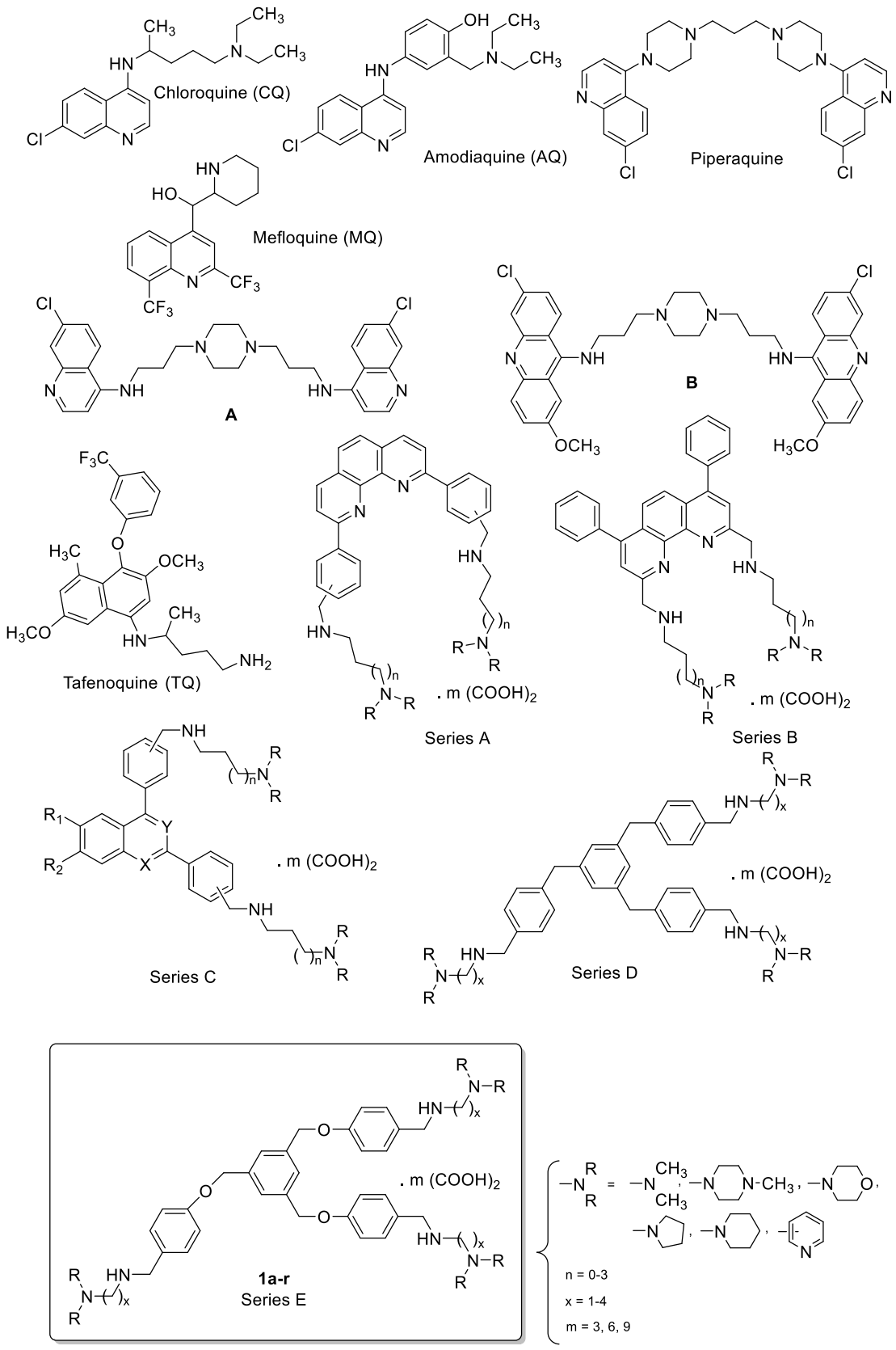

Figure 1. The structures of chloroquine (CQ), amodiaquine (AQ), piperaquine, mefloquine (MQ), bisquinoline (**A**), bisacridine (**B**), tafenoquine, series (**A**–**D**), and newly synthesized 1,3,5-*tris*[(4-(substituted-aminomethyl)phenoxy)methyl]benzene derivatives **1a–r** (Series (**E**)).

In our research endeavors, we concentrated on the exploration of novel nitrogen heterocyclic compounds with potential applications in antiprotozoal chemotherapy [14–22]. Previously, we have designed various series, including 2,9-*bis*[(substituted-aminomethyl)phenyl] phenanthrolines (series A-B), 2,4-*bis*[(substituted-aminomethyl)phenyl]quinoline, 1,3-bis [(substituted-aminomethyl)phenyl]isoquinoline, and 2,4-*bis*[(substituted-aminomethyl) phenyl]quinazoline derivatives (series C) [16,19–22]. More recently, we have developed a new series of 1,3,5-*tris*[(4-(substituted-aminomethyl)phenyl)methyl]benzene derivatives (series D), which could be considered as a novel alternative antiparasitic scaffold. These novel series D were developed as potential candidates for antiprotozoal agents, specifically designed to interact with *Plasmodium falciparum* DNA G-quadruplexes via π-stacking interactions [23]. Synthetic access to these C-3 homo-trimeric ligands has led to drug candidates with an aesthetic structure but with promising antimalarial activity. Thus, these new compounds could offer the possibility of binding DNA G-4 more efficiently. In fact, DNA G-quadruplex as a therapeutic target could also take advantages of these C3-symmetric ligands for better interactions and therapeutic effects [24].

This design aims to overcome resistance mechanisms employed by parasites, including drug efflux. It has been previously documented that the telomeres of various protozoa could serve as attractive drug targets [25–28]. Telomerase activity is observed in gametocytes and during the transition to the erythrocytic stage of the *P. falciparum* parasite [29,30]. The telomeric 3′ G-overhang region of *P. falciparum* consists of a repetitive degenerate unit 5′GGGTTYA3′ (where Y could be T or C) [31], which can fold into intramolecular G-quadruplex and can modulate expression of a G-quadruplex-containing reporter gene [32]. Hence, it has been previously described that different G-quadruplex-binding drugs were potent and fast-acting against the intraerythrocytic stages of the parasite in vitro [30,32]. Notably, this variation between parasitic and human (5′GGGTTA3′) G-quadruplexes suggests the potential for developing antiprotozoal ligands specifically targeting the G-quadruplexes present in this parasitic species.

Given our research expertise in the preparation of novel antiprotozoal heterocyclic derivatives, we present here the design and synthesis of original 1,3,5-*tris*[(4-(substituted-aminomethyl) phenoxy)methyl]benzenes derivatives **1** (Series E) that could be considered as novel structural analogues of our previously described 1,3,5-*tris*[(4-(substitutedaminomethyl)phenyl)methyl] benzenes (Series D). These new compounds represent a unique and promising antiparasitic scaffold for combating malaria. Our hypothesis is based on the idea that introducing three diaminophenoxy moieties at positions 1, 3, and 5 of the benzene ring could result in more flexible and potent G4 ligands with increased selectivity, achieved through the expansion of the distance between the aromatic moieties.

We anticipate that the extended aromatic moieties of the diaminophenoxy groups will facilitate π–π stacking interactions with various G-quartets, the classical strategy and mechanism to stabilize G-quadruplexes.

We examine the in vitro antiprotozoal activities of these new compounds against both the chloroquine-sensitive (3D7) and chloroquine-resistant (W2) strains of the malaria parasite *Plasmodium falciparum*. The in vitro cytotoxicity of our 1,3,5-*tris*[(4-(substituted-aminomethyl)phenoxy)methyl]benzene derivatives **1** was assessed in human HepG2 cells. For each compound, we determine the index of selectivity and the ratio of cytotoxicity to antiprotozoal activity. Furthermore, we explore whether these innovative polyaromatic compounds have the potential to stabilize certain parasitic telomeric DNA G-quadruplex structures. The assessment of the potential stabilization of *Plasmodium falciparum* telomeric G-quadruplexes is conducted using a FRET melting assay.

2. Results and Discussion

2.1. Chemistry

The new 1,3,5-*tris*[(4-(substituted-aminomethyl)phenoxy)methyl]benzene derivatives **1a–r** were synthesized by initiating the process with commercially available 1,3,5-*tris*(bromomethyl)benzene (Scheme 1). The intermediate stage involved the creation of 1,3,5-*tris*

[(4-formylphenoxy)methyl]benzene **2** through a coupling reaction between 1,3,5-*tris*(bromomethyl)benzene and an excess of 4-hydroxybenzaldehyde in the presence of potassium carbonate in THF [33,34]. The structure of intermediate compound **2** was established by X-ray crystallography (Figure 2) [35].

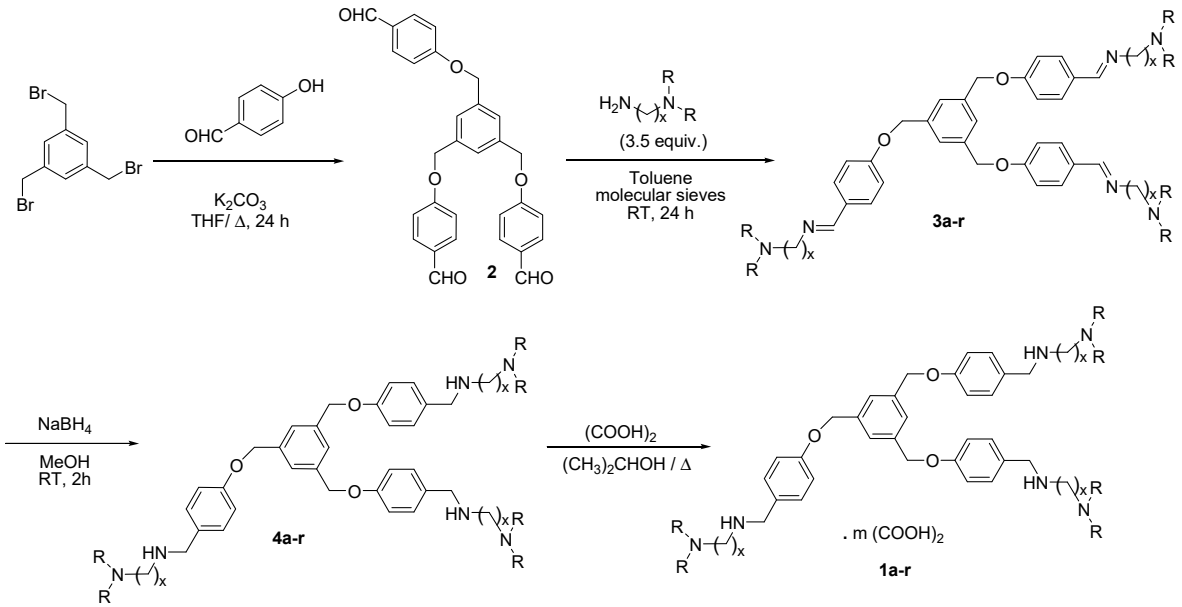

		x	m
3a, 4a, 1a	$-N(CH_3)_2$	2	6
3b, 4b, 1b	$-N(CH_3)_2$	3	6
3c, 4c, 1c	$-N(CH_3)_2$	4	6
3d, 4d, 1d	$-N$ N-CH_3	2	9
3e, 4e, 1e	$-N$ N-CH_3	3	9
3f, 4f, 1f	$-N$ O	3	6
3g, 4g, 1g	$-N$	3	6
3h, 4h, 1h	$-N$	3	6
3i, 4i, 1i	N	0	3

		x	m
3j, 4j, 1j	N	1	3
3k, 4k, 1k	N	2	3
3l, 4l, 1l	N	3	3
3m, 4m,1m	N	1	3
3n, 4n, 1n	N	2	3
3o, 4o, 1o	N	3	3
3p, 4p, 1p	N	1	3
3q, 4q, 1q	N	2	3
3r, 4r, 1r	N	3	3

Scheme 1. General procedure for the preparation of novel compounds **1a–r**.

Subsequently, the reaction of various primary-substituted alkylaminoalkylamines with this trialdehyde **2** resulted in the formation of 1,3,5-*tris*[(4-(substituted-iminomethyl)phenoxy) methyl]benzenes **3a–r**, which were then reduced to yield the derivatives **4a–r**, namely, 1,3,5-*tris*[(4-(substituted-aminomethyl)phenoxy)methyl]benzenes, using sodium borohydride in methanol, following a previously established procedure by our team [16,19,21–23]. These novel derivatives **4a–r** (Figures S1–S18) were then converted into ammonium oxalate salts **1a–r** through a reaction with oxalic acid in reflux isopropanol. These compounds were converted into oxalates to require water solubility parameters for biological testing. These oxalate salts were found to be less hygroscopic than the hydrochloride ones and were also soluble in water. Table 1 provides the physical properties of these newly ammonium oxalates **1a–r**.

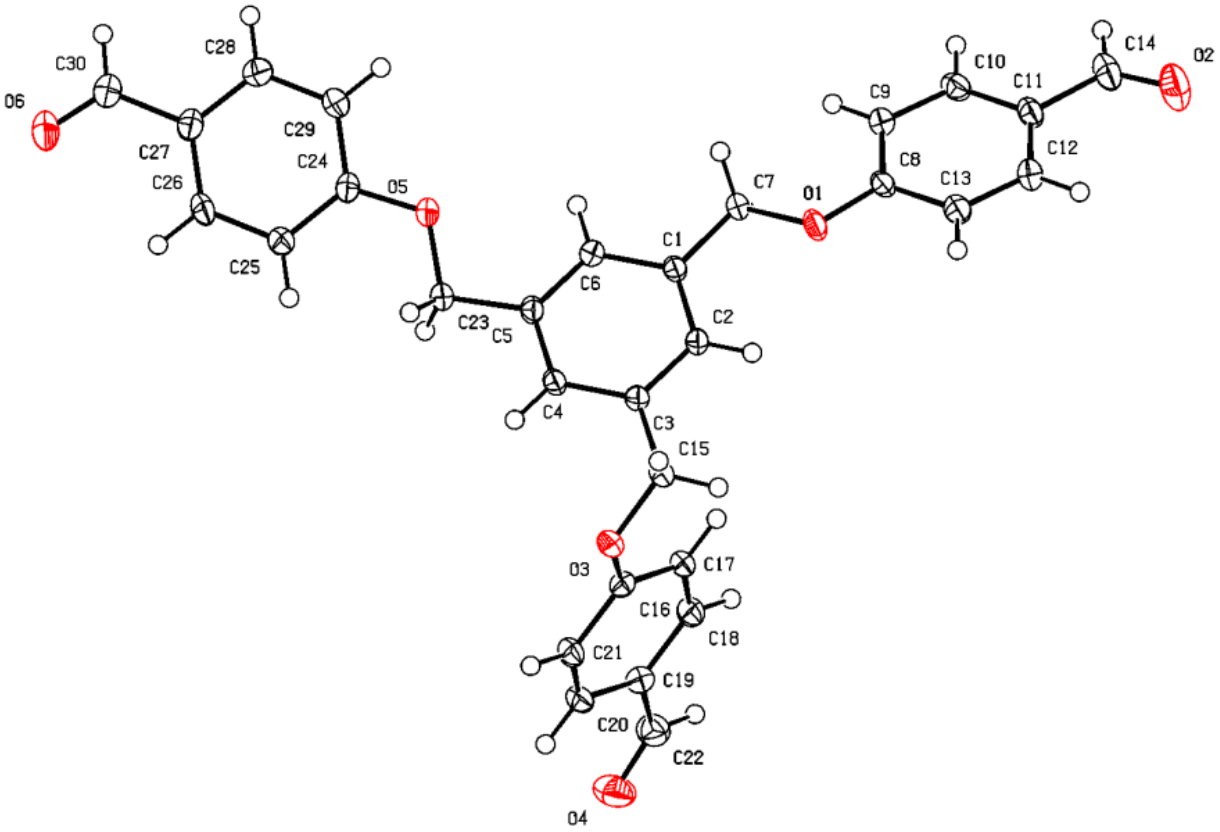

Figure 2. The ORTEP (Oak Ridge Thermal Ellipsoid Plot) drawing of the 1,3,5-*tris*[(4-formylphenoxy) methyl]benzene **2** with atom labeling and thermal ellipsoids at 30% probability level. Hydrogen atoms are represented as small spheres of arbitrary radii.

Table 1. Physical properties of ammonium oxalate salts **1a–r**.

Compound		Salt [a]	Melting Point (°C) [b]	% Yield [c]
1a	Beige crystals	6 $(COOH)_2$	245–247	57.1
1b	Grey crystals	6 $(COOH)_2$	147–149	70.1
1c	White crystals	6 $(COOH)_2$	189–191	49.8
1d	White crystals	9 $(COOH)_2$	235–237	59.8
1e	White crystals	9 $(COOH)_2$	243–245	55.7
1f	White crystals	6 $(COOH)_2$	178–180	77.5
1g	Yellow crystals	6 $(COOH)_2$	225–227	72.1
1h	White crystals	6 $(COOH)_2$	193–195	79.3
1i	Yellow crystals	3 $(COOH)_2$	173–175	60.4
1j	Beige crystals	3 $(COOH)_2$	239–141	77.5
1k	Yellow crystals	3 $(COOH)_2$	173–175	77.1
1l	Yellow crystals	3 $(COOH)_2$	177–179	89.2
1m	White crystals	3 $(COOH)_2$	259–261	83.4
1n	Beige crystals	3 $(COOH)_2$	248–250	69.2
1o	Yellow crystals	3 $(COOH)_2$	185–187	86.6
1p	Grey crystals	3 $(COOH)_2$	227–229	45.8
1q	Beige crystals	3 $(COOH)_2$	191–193	78.5
1r	White crystals	3 $(COOH)_2$	151–153	89.3

[a] The stoichiometry and composition of the salts were determined using elemental analyses, and obtained values were within ±0.4% of the theoretical values. [b] Crystallization solvent: 2-PrOH–H_2O. [c] The total yields included the conversions into the ammonium oxalates starting from commercially available 1,3,5-*tris*(bromomethyl)benzene.

2.2. Biological Evaluation

2.2.1. In Vitro Antimalarial Activity

All these new 1,3,5-*tris*[(4-(substituted-aminomethyl)phenoxy)methyl]benzene derivatives **1a–r** were tested for their in vitro antimalarial activity by incubation with *P. falciparum* chloroquine (CQ)-resistant strain W2 (IC_{50} CQ = 0.40 µM, IC_{50} mefloquine (MQ) = 0.016 µM) and the strain 3D7, which is CQ-sensitive and has decreased sensitivity to MQ (IC_{50} CQ = 0.11 µM, MQ = 0.06 µM). The IC_{50} values of these original bioactive 1,3,5-*tris*[(4-(substituted-aminomethyl)phenoxy)methyl]benzenes **1a–r** were observed between 0.07 and greater than 40 µM against the CQ-resistant strain W2 and between 0.06 and greater than 40 µM against the 3D7 *P. falciparum* strains (Table 2).

Table 2. In vitro sensitivity of *P. falciparum* strains to compounds **1a–r** and cytotoxicity of these derivatives in HepG2 cells.

Compound	*P. falciparum* Strains IC_{50} Values (µM) [a]		Cytotoxicity to HepG2 Cells CC_{50} Values (µM) [b]	Resistance Index	
	W2	3D7		W2 [e]	3D7 [f]
CQ [c]	0.40 ± 0.04	0.11 ± 0.01	30	3.64	0.28
MQ [c]	0.016 ± 0.002	0.06 ± 0.003	n.d. [d]	0.27	3.75
1a	n.d. [d]	0.35 ± 0.07	0.11 ± 1.50	n.d. [d]	n.d. [d]
1b	14.88 ± 0.83	4.57 ± 0.65	66.25 ± 2.10	3.26	0.31
1c	>40	18.94 ± 1.32	26.21 ± 2.48	>2.11	0.47>
1d	>40	>40	32.46 ± 0.45	n.d. [d]	n.d. [d]
1e	>40	>40	58.53 ± 1.90	n.d. [d]	n.d. [d]
1f	>40	>40	13.80 ± 0.74	n.d. [d]	n.d. [d]
1g	>40	>40	8.16 ± 0.55	n.d. [d]	n.d. [d]
1h	>40	11.01 ± 0.96	49.50 ± 1.33	>3.63	0.28>
1i	>40	>40	>100	n.d. [d]	n.d. [d]
1j	0.08 ± 0.04	0.09 ± 0.06	2.45 ± 0.60	0.89	1.13
1k	0.74 ± 0.41	0.89 ± 0.15	3.75 ± 0.42	0.83	1.20
1l	2.08 ± 0.52	0.62 ± 0.17	2.66 ± 0.31	3.35	0.30
1m	0.07 ± 0.04	0.06 ± 0.10	62.11 ± 2.31	1.17	0.86
1n	0.74 ± 0.20	0.19 ± 0.08	2.46 ± 0.36	3.89	0.26
1o	0.41 ± 0.22	1.94 ± 0.77	0.16 ± 0.07	0.21	4.73
1p	0.17 ± 0.31	0.08 ± 0.02	3.86 ± 0.78	2.13	0.47
1q	0.29 ± 0.07	0.12 ± 0.06	0.72 ± 0.23	2.42	0.41
1r	0.48 ± 0.09	0.35 ± 0.05	0.18 ± 0.12	1.37	0.73

[a] Values were measured against CQ-resistant and mefloquine-sensitive strain W2 and the CQ-sensitive and MQ decreased sensitivity strain 3D7. The IC_{50} (µM) values correspond to the means +/− standard deviations from three independent experiments. [b] CC_{50} values were measured against HepG2 cells. The CC_{50} (µM) values correspond to the means +/− standard deviations from three independent experiments. [c] CQ and MQ were used as antiplasmodial compounds of reference. [d] n.d.: not determined. [e] IC_{50} (W2)/IC_{50} (3D7). [f] IC_{50} (3D7)/IC_{50} (W2).

In this new original series, it can be observed that 1,3,5-*tris*[(4-(substituted-aminomethyl) phenoxy) methyl]benzenes **1k–r** bearing pyridinylalkylaminomethyl side chains at position 4 of the methylphenoxy nucleus displayed better activities than their analogues substituted with alkylaminoalkylaminomethyl side chains (compounds **1a–h**) against the W2 strain; the IC_{50} of compounds **1k–r** were noticed ranging from 0.07 to 2.08 µM in comparison with IC_{50} of 14.88 to >40 µM for **1a–h**. Indeed, in the subseries of derivatives bearing alkylaminoalkylaminomethyl side chains (compounds **1a–h**), only 1,3,5-*tris* [(4-(3-dimethylaminopropyl)aminomethyl)phenoxy)methyl]benzene **1b** showed moderate antimalarial activity against the W2 strain with an IC_{50} of 14.88 µM. In addition, the 1,3,5-*tris* [(4-(pyridin-3-ylmethylaminomethyl)phenoxyl)methyl]benzene **1m** was found to be the most active compound against the W2 strain in this pyridinyl substituted subseries with an IC_{50} of 0.07 µM. Always in this pyridinylalkylamino-substituted subseries (compounds **1j–r**), it can be noticed that the substitution of the side chains by C_1 alkyl chains showed better antimalarial activities against the W2 strain than their C_2 homologs, for example,

IC_{50} = 0.07 μM for **1m** in comparison with 0.74 μM for **1n**, or 0.17 μM for **1p** *versus* 0.29 μM for **1q**.

Against the 3D7 CQ-sensitive strain, the three 1,3,5-*tris*[(4-(pyridinylmethylaminomethyl)phenoxy)methyl]benzene **1j**, **1m,** and **1p** substituted by three pyridinylmethylaminomethyl side chains at position 4 of each of the phenoxy groups were found to be the most active derivative with IC_{50} of 0.09, 0.06, and 0.08 μM, respectively. Moreover, from a structure–activities relationships point of view, the same observations were made as those found for the W2 strain. Concerning our compounds **1a–h** bearing alkylaminoalkylaminomethyl side chains, some antimalarial activities were observed between 0.35 and 18.94 μM against the 3D7 *P. falciparum* strain (compounds **1a–c** and **1h**), while the other ones were found to be inactive with IC_{50} greater than 40 μM (compounds **1d–g**). In addition, concerning compounds **1a–c**, the substitution of the side chains by C_2 alkyl chains showed better antimalarial activities against the 3D7 strain than their C_3 or C_4 homologs, i.e., IC_{50} 0.35 μM for **1a** in comparison with 4.57 and 18.94 μM for **1b** and **1c**, respectively.

Curiously, the new derivative **1i** bearing three quinoline heterocycles, with a nucleus found in the reference molecules CQ and MQ, did not show any antimalarial activity against the CQ-sensitive and MQ-resistant *P. falciparum* strain 3D7 and against the CQ-resistant and mefloquine-sensitive *P. falciparum* strain W2.

The resistance index values (Table 3), defined as the ratio of the IC_{50} of the resistant line to that of the sensitive strain, were also calculated in relation to the activities at the level of a strain resistant to CQ (W2) and a strain with reduced sensitivity to MQ (3D7). For CQ, the W2/3D7 ratio is close to ~3.64. Since strain W2 is resistant to CQ and 3D7 is sensitive to CQ, this value (~3.64) is an indication of the level of specific CQ resistance observed. Any compound with a W2/3D7 ratio >3.64 is more resistant to W2 than CQ, indicating a shared mechanism of action. From the data in Table 2, it appears that compounds **1b** (W2/3D7~3.26), **1h** (>3.63), **1l** (~3.35), and **1n** (~3.9) could all share the CQ mechanism of action. Similarly, for MQ, the 3D7/W2 ratio is ~ 3.75. Since 3D7 has reduced sensitivity to MQ, compound that has a 3D7/W2 ratio > 3.75 may share a mechanism of action with MQ. Compound **1o** presented a 3D7/W2 ratio of 4.73. Further investigations should now be realized to determine their mode of action.

Table 3. Selectivity indices (SI [a]) of compounds **1a–r** [a].

Compound	HepG2/W2	HepG2/3D7
CQ	75	272
1a	n.d. [b]	0.32
1b	4.45	14.50
1c	n.d. [b]	1.38
1d	n.d. [b]	n.d. [b]
1e	n.d. [b]	n.d. [b]
1f	n.d. [b]	n.d. [b]
1g	n.d. [b]	n.d. [b]
1h	n.d. [b]	4.50
1i	n.d. [b]	n.d. [b]
1j	30.63	27.22
1k	5.07	4.21
1l	1.28	4.29
1m	887.29	1035.17
1n	3.32	12.95
1o	0.39	0.08
1p	22.71	48.25
1q	2.48	6.00
1r	0.38	0.51

[a] SI was defined as the ratio between the CC_{50} value on the HepG2 cells and the IC_{50} value against the *P. falciparum* W2 or 3D7 strains. [b] n.d.: not determined.

2.2.2. Cytotoxicity and Selectivity Index

In order to assess their selectivity of action, the cytotoxicities of our new antimalarial 1,3,5-*tris*[(4-(substituted-aminomethyl)phenoxy)methyl]benzenes **1a–r** were evaluated in vitro on the human cell line HepG2, a commonly used human-derived hepatocarcinoma cell line that expresses many hepatocyte-specific metabolic enzymes. In addition to revealing the possible cytotoxic nature of a tested compound, this assay can also detect the formation of toxic metabolites without, however, allowing their identification, making HepG2 a particularly discriminating cell line in terms of assessing the in vitro cytotoxicity of original compounds [36,37]. The cytotoxic concentrations of 50% (CC_{50}) were determined, and selectivity indexes (SIs), defined as the ratios of cytotoxic to antiparasitic activities ($SI = CC_{50}/IC_{50}$), were calculated (Table 3).

Our new 1,3,5-*tris*[(4-(substituted-aminomethyl)phenoxy)methyl]benzene derivatives **1a–r** showed cytotoxicity against these HepG2 cells with CC_{50} values ranging from 0.16 to 71.04 μM. Against this human cell line HepG2, the 1,3,5-*tris*[(4-(substituted-aminomethyl) phenoxy)methyl]benzenes substituted by three pyridinylalkylaminomethyl side chains (compounds **1j–r**) were found to be more cytotoxic, except compound **1m** (CC_{50} = 62.11 μM), than their analogs substituted with three alkylaminoalkylaminomethyl side chains (compounds **1a–h**), i.e., CC_{50} = 0.16 to 3.86 μM for **1j–r** versus CC_{50} = 8.16 to 71.04 μM for **1a–h**. Moreover, compound **1i**, substituted by three quinoline rings on its side chains, showed a CC_{50} > 100 μM.

Concerning the *P. falciparum* strain W2, the calculated SIs were noticed to be between 0.38 and 887.29. For the CQ-sensitive strain 3D7, the SIs were noticed to be from 0.08 to 1035.17. These SI data led us to identify the 1,3,5-*tris*[(4-(substituted-aminomethyl)phenoxy) methyl]benzene **1m** as the most promising antimalarial compound with an SI of 887.29 and 1035.17 for the *P. falciparum* W2 and 3D7 strains. In addition, we can notice that its previously described structural homolog of the series D also presented a very interesting selectivity index on the *P. falciparum* 3D7 strain; however, this latter compound showed to be significantly less promising than this new synthesized derivative **1m**, i.e., SI = 83.7 for analogue of series D versus SI = 1035.2 for **1m** in series E. In addition, derivative **1p**, a structural homolog of compound **1m**, but substituted by three pyridine-4-ylmethylamino side chains, was also identified as an interesting antimalarial compound with SI of 22.71 and 48.25 against the W2 and 3D7 strains, respectively (Figure 3).

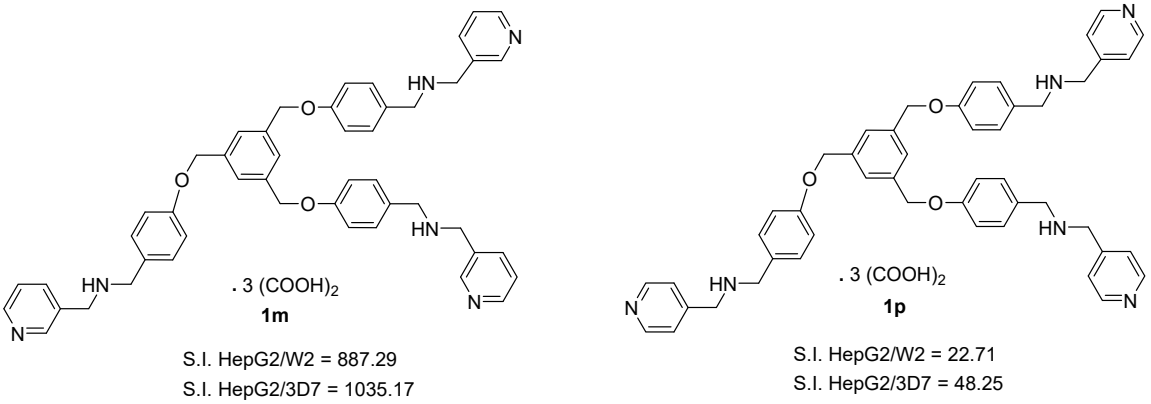

Figure 3. The structures of the most promising synthesized 1,3,5-*tris*[(4-(substituted-aminomethyl) phenoxy)methyl]benzene derivatives **1m** and **1p**. Selectivity indexes (S.I.) are provided below.

These very interesting SI values could indicate that these novel original 1,3,5-*tris* [(4-(substituted-aminomethyl)phenoxy)methyl]benzene compounds **1** warrant further investigations into their potential use as antimalarial drugs.

2.3. FRET Melting Experiments

Considering the potential of *P. falciparum* telomeres as promising targets for polyaromatic derivatives [22,29,31,32], we further explored the capability of biologically active compounds **1** to potentially stabilize *P. falciparum* telomeric chromosomal G-quadruplexes. This investigation was conducted using a FRET melting assay. The aim was to assess the extent to which the novel polyaromatic derivatives **1** could stabilize G-quadruplex structures formed by oligonucleotides with sequences derived from both *P. falciparum* and human telomeres. Two fluorescently labelled *P. falciparum* telomeric chromosomal sequences (FPf1T and FPf8T) and one human telomeric sequence (F21T) were used in this assay.

To probe the G4 selectivity of our novel 1,3,5-*tris*[(4-(substituted-aminomethyl)phenoxy) methyl]benzene ligands **1** over duplex DNA, a FRET melting assay was performed using a hairpin duplex control sequence, FdxT. In comparison, we also evaluated a reference G4 ligand, PhenDC3 (not active against *P. falciparum*), and the antimalarial reference drugs, CQ and MQ. Comparatively in this assay, we also used as reference the FRET data found for our best ligand synthesized in series D, the 1,3,5-*tris*[(4-(substituted-aminomethyl)phenyl)methyl]benzene ligand **1'd**. To facilitate a meaningful comparison of selectivities, we calculated the difference (ΔTm) between the melting temperature (Tm) of the G-quadruplex formed by FPf1T, FPf8T, F21T, or FdxT in the presence or absence of each selected derivative. These ΔTm values are summarized in Table 4, with the selected ligands **1** exhibiting ΔTm values ranging from 0.43 to 40.39 °C at a 2 μM derivative concentration.

Table 4. FRET melting values for compounds **1a–r** (2 μM) with FPf1T, FPf8T, F21T, and FdxT (0.2 μM) in K^+ conditions.

Compound	ΔTm (°C) [a] FPf1T			ΔTm (°C) [a] FPf8T			ΔTm (°C) [a] F21T			ΔTm (°C) [a] FdxT		
PhenDC3	21.92	±	3.30	26.48	±	1.66	22.28	±	0.52	0.83	±	0.04
CQ	1.90	±	0.10	2.40	±	1.20	2.40	±	1.10		n.d. [b]	
MQ	3.10	±	0.50	6.60	±	2.30	2.60	±	0.50		n.d. [b]	
1'd in series D	23.1	±	0.4	24.30	±	1.50	22.40	±	3.30		3.10 ± 0.3	
1a	12.72	±	0.14	15.70	±	2.57	11.41	±	0.02	0.71	±	0.03
1b	27.61	±	0.40	26.16	±	1.46	22.56	±	1.19	5.06	±	0.08
1c	37.83	±	0.40	40.39	±	1.34	33.33	±	0.21	12.61	±	0.24
1d	21.75	±	1.15	24.97	±	2.28	20.45	±	0.29	3.00	±	0.39
1e	24.48	±	0.93	25.53	±	0.06	18.68	±	3.52	3.42	±	0.01
1f	20.94	±	10.20	18.90	±	9.46	12.20	±	0.10	0.69	±	0.05
1g	24.41	±	2.32	24.61	±	0.57	17.91	±	1.76	3.46	±	0.19
1h	18.41	±	3.04	15.71	±	0.08	12.27	±	0.99	0.93	±	0.34
1i	−0.69	±	0.08	−0.20	±	0.55	−0.33	±	0.19	0.09	±	0.04
1j	8.39	±	0.56	5.05	±	1.06	3.06	±	0.03	−0.05	±	0.71
1k	5.40	±	0.44	9.31	±	0.37	7.74	±	0.16	0.29	±	0.03
1l	10.92	±	1.00	16.80	±	0.46	13.82	±	0.83	0.53	±	0.08
1m	8.94	±	1.01	12.23	±	0.28	9.68	±	0.34	0.31	±	0.06
1n	8.61	±	1.22	12.15	±	2.55	10.06	±	2.32	0.16	±	0.08
1o	14.44	±	2.78	20.24	±	2.26	16.49	±	0.48	1.18	±	0.02
1p	1.33	±	0.20	1.50	±	0.06	0.43	±	0.25	−0.03	±	0.22
1q	8.36	±	0.66	12.18	±	1.22	10.11	±	1.26	0.29	±	0.15
1r	12.14	±	0.98	15.78	±	0.19	12.88	±	0.78	0.57	±	0.19

[a] ΔT_m of FPf1T, FPf8T, F21T, and FdxT (0.2 μM) were recorded in 10 mM lithium cacodylate (pH 7.2), 10 mM KCl, and 90 mM LiCl. PhenDC3 was tested at 0.5 μM, whereas CQ and MQ were tested at 1 μM. Error margins correspond to SD of three replicates. [b] n.d.: not determined.

Compounds **1b** and **1c** were found to be the best 1,3,5-*tris*[(4-(substituted-aminomethyl) phenoxy)methyl]benzene ligands, which stabilized the three G-quadruplexes sequences (the two parasitic FPf1T and FPf8T, and the human F21T) with ΔTm values ranging from 22.56 to 40.39 °C (Table 4). In terms of structure–activity relationships, we could notice that the polyaromatic derivatives substituted with various alkylaminoalkylaminomethyl side chains (compounds **1a–h**) strongly stabilize the FPf1T, FPf8T, and F21T G-quadruplexes. The ΔTm values ranged from 11.41 to 40.39 °C at a 2 μM ligand concentration. Still concern-

ing compounds **1a–h**, these stabilized the FPf1T and FPf8T G-quadruplexes to a slightly greater extent than they did the human F21T G-quadruplex. These preliminary results mean that most of the tested derivatives **1a–h** substituted with different alkylaminoalkylaminomethyl side chains have a moderate preference for *Plasmodium* over human telomeric quadruplexes. In addition, all our ligands **1a–r** were also found to be more specific for FPf8T with higher ΔTm for FPf8T than for F21T. This remark is not applicable to the FPf1T sequence since a certain number of compounds (**1k–o** and **1q–r**) presented higher ΔTm for F21T in comparison of those found for FPf1T (Figure 4).

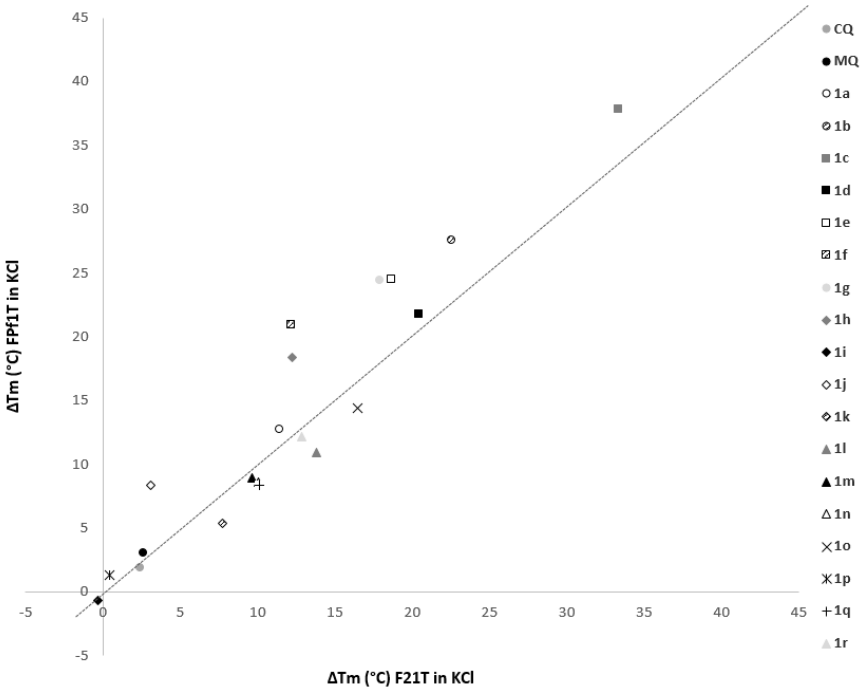

(**A**)

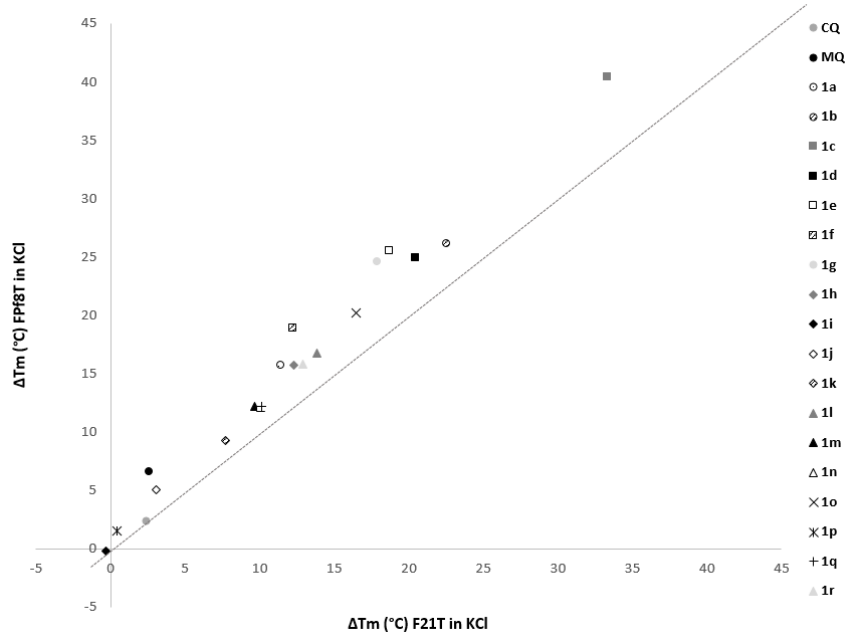

(**B**)

Figure 4. Thermal stabilization (ΔTm) induced by selected compounds **1a–r** (at 2 μM) of *Plasmodium* telomeric G-quadruplexes (**A**) FPf1T and (**B**) FPf8T vs. the human telomeric quadruplex F21T.

Moreover, most of the 1,3,5-*tris*[(4-(substituted-aminomethyl)phenoxy)methyl]benzenes substituted by three pyridinylalkylaminomethyl chains (compounds **1j–r**) or bearing three quinolinylaminomethyl chains (derivative **1i**) exhibited a lower stabilization profile on the two *Plasmodium* telomeric sequences (FPf1T and FPf8T) and the human one (F21T) in comparison with their alkylaminoalkylaminomethyl substituted analogs **1a–h**; i.e., ΔTm values for **1i–r** were noticed ranging from −0.20 to 20.24 °C, although the 1,3,5-*tris*[(4-(pyridinylalkylaminomethyl)phenoxy)methyl]benzenes **1j–r** demonstrated the best antimalarial activities against both *P. falciparum* W2 and 3D7 strains.

The radar plot presented in Figure 5 shows that the compounds **1a–r** may be able to more or less stabilize some of the G4 forming sequences.

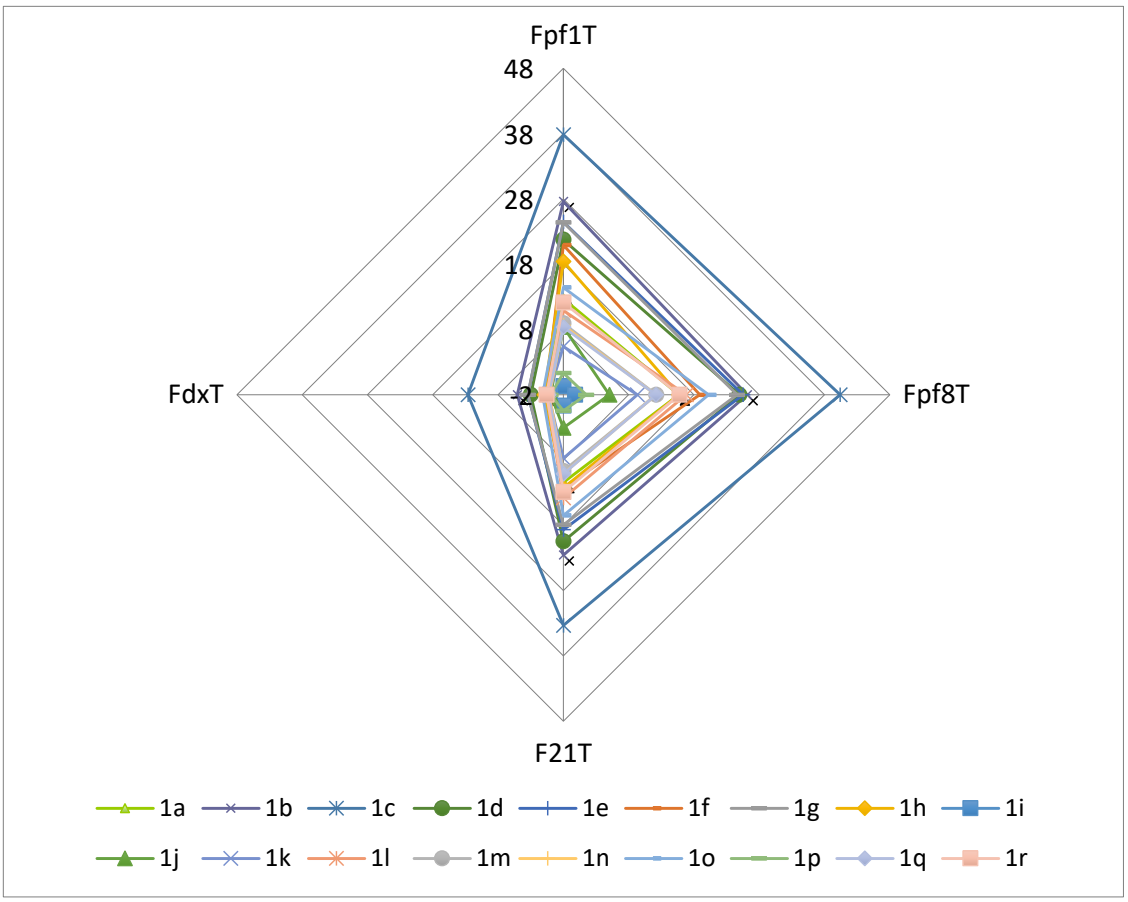

Figure 5. Stabilization specificity profile of **1a–r** (2 μM) toward various G4 and control duplex oligonucleotides. The difference in Tm in presence and absence of **1a–r**, ΔTm, in °C is plotted for each sequence. Three quadruplexes and one duplex (FdxT) were tested.

Little or no binding to the duplex DNA sequence was detected by using FRET assays, excepted compound **1c**, which showed a ΔTm of 12.61 °C.

In terms of stabilizing the protozoal G-quadruplex, it was noted that the most promising 1,3,5-*tris*[(4-(substituted-aminomethyl)phenoxy)methyl]benzenes **1a–h**, which demonstrated a noteworthy stabilization profile, did not rank as the most effective antimalarial derivatives against the two *Plasmodium* strains. Consequently, no significant correlations were observed between their antimalarial activities and the selectivity of their binding to G-quadruplexes. These derivatives of 1,3,5-*tris*[(4-(substituted-aminomethyl)phenoxy)methyl]benzene are unlikely to exhibit specific cytotoxicity through mechanisms involving G-quadruplex binding. The same remark has been considered for our previously described series D. Moreover, it would be interesting to broaden the pharmacological evaluation of our new derivatives **1** by investigating their potential modes of action through further studies.

3. Materials and Methods

3.1. Chemistry

3.1.1. General

Commercially available reagents were used without additional purification. Melting points were determined with an SM-LUX-POL Leitz hot-stage microscope (Leitz GMBH, Midland, ON, USA) and are uncorrected.

IR spectra were recorded on a NICOLET 380FT-IR spectrophotometer (Bruker BioSpin, Wissembourg, France). NMR spectra were recorded with tetramethylsilane as an internal standard using a BRUKER AVANCE 300 spectrometer (Bruker BioSpin, Wissembourg, France). Splitting patterns have been reported as follows: s = singlet; bs = broad singlet; d = doublet; t = triplet; q = quartet; dd = double doublet; ddd = double double doublet; qt = quintuplet; and m = multiplet.

Analytical TLC were carried out on 0.25 precoated silica gel plates (POLYGRAM SIL G/UV254) (Merck KGaA, Darmstadt, Germany) and compounds were visualized after UV light irradiation. A silica gel 60 (70–230 mesh) was used for column chromatography. Mass spectra were recorded on an ESI LTQ Orbitrap Velos mass spectrometer (ThermoFisher, Bremen, Germany). Ionization was performed using an Electrospray ion source operating in positive ion mode with a capillary voltage of 3.80 kV and capillary temperature of 250 °C. The scan type analyzed was full scan, all MS recordings were in the m/z range between 150 and 2000 m/z. No fragmentation was carried out and the resolution used for the analysis was 60,000.

3.1.2. Synthesis of the 1,3,5-*Tris*[(4-Formylphenoxy)Methyl]Benzene **2**

To a suspension of 1,3,5-*tris*(bromomethyl)benzene (2.5 mmol), 4-hydroxybenzaldehyde (10 mmol) in THF (40 mL), 17.5 mmol of powder K_2CO_3 was added. The reaction mixture was refluxed for 24 h. The suspension was then filtered, evaporated to dryness, and extracted with DCM (2 × 30 mL). The organic layer was filtered and washed with a solution of NaOH 2.5 M (2 × 20 mL). The organic layer was dried over sodium sulfate, filtered, and evaporated under reduced pressure to give the pure product **2**. White crystals (93%); Mp = 142–144 °C [33,34]. ^{1}H NMR ($CDCl_3$) δ ppm: 9.89 (s, 3H, CHO), 7.89 (d, 6H, J = 8.10 Hz, H-3$_{phen}$ and H-5$_{phen}$), 7.10 (d, 6H, J = 8.10 Hz, H-2$_{phen}$ and H-6$_{phen}$), 7.51 (s, 3H, H$_{benz}$), 5.21 (s, 6H, CH_2); ^{13}C NMR ($CDCl_3$) δ ppm: 192.1 (CO), 164.8 (C-4$_{phen}$), 138.7 (Cq-$_{benz}$), 133.4 (C-3$_{phen}$ and C-5$_{phen}$), 132.3 (C-1$_{phen}$), 127.8 (CH$_{benz}$), 116.5 (C-2$_{phen}$ and C-6$_{phen}$), 71.1 (CH_2). A yellow single crystal of **2** was obtained by slow evaporation from a methanol/chloroform solution (v/v: 20/80): triclinic, space group P-1, a = 7.5959(17) Å, b =13.128(3) Å, c = 13.412(3) Å, α = 118.716(13)°, β = 94.568(4)°, γ = 93.795(4)°, V = 1160.8(5) Å^3, Z = 2, δ(calcd) = 1.375 Mg.m^{-3}, FW = 480.49 for $C_{30}H_{24}O_6$, F(000) = 504.0. Full crystallographic results were deposited at the Cambridge Crystallographic Data Centre (CCDC-2358055), UK, as shown in the supplementary X-ray crystallographic data [35].

3.1.3. General Procedure for the Synthesis of 1,3,5-*Tris*[(4-(Substituted-Iminomethyl) Phenoxy)Methyl]Benzenes **3a–r**

The 1,3,5-*tris*[(4-formylphenoxy)methyl]benzene **2** (100 mg, 0.2 mmol) was dissolved in 6 mL of toluene. Activated molecular sieves 4 Å (800 mg) were introduced followed by dialkylamine (0.7 mmol). The reaction mixture was stirred for 24 h. The suspension obtained was filtered, washed with dichloromethane, and the solvent was removed under reduced pressure to afford the tri-imine **3**. The crude products were then used without further purification.

1,3,5-*Tris*[(4-(2-dimethylaminoethyl)iminomethyl)phenoxy)methyl]benzene (**3a**)

Yellow oil (99%); ^{1}H NMR ($CDCl_3$) δ ppm: 8.23 (s, 3H, CH=N), 7.68 (d, 6H, J = 8.10 Hz, H-3$_{phen}$ and H-5$_{phen}$), 6.99 (d, 6H, J = 8.10 Hz, H-2$_{phen}$ and H-6$_{phen}$), 7.45 (s, 3H, H$_{benz}$), 5.10 (s, 6H, CH_2), 3.71 (t, 6H, J = 6.90 Hz, NCH_2), 2.62 (t, 6H, J = 6.90 Hz, NCH_2), 2.30 (s, 18H, $N(CH_3)_2$).

1,3,5-*Tris*[(4-(3-dimethylaminopropyl)iminomethyl)phenoxy)methyl]benzene (**3b**)

Yellow oil (98%); ^{1}H NMR ($CDCl_3$) δ ppm: 8.20 (s, 3H, CH=N), 7.67 (d, 6H, J = 8.10 Hz, H-3$_{phen}$ and H-5$_{phen}$), 7.64 (s, 3H, H$_{benz}$), 6.98 (d, 6H, J = 8.10 Hz, H-2$_{phen}$ and H-6$_{phen}$), 5.08 (s, 6H, CH_2), 3.60 (t, 6H, J = 6.90 Hz, NCH_2), 2.34 (t, 6H, J = 6.90 Hz, NCH_2), 2.22 (s, 18H, $N(CH_3)_2$), 1.85 (qt, 6H, J = 8.40 Hz, CH_2).

1,3,5-*Tris*[(4-(4-dimethylaminobutyl)iminomethyl)phenoxy)methyl]benzene (**3c**)

Yellow oil (98%); ^{1}H NMR ($CDCl_3$) δ ppm: 8.15 (s, 3H, CH=N), 7.61 (d, 6H, J = 8.1 Hz, H-3$_{phen}$ and H-5$_{phen}$), 7.41 (s, 3H, H$_{benz}$), 6.94 (d, 6H, J = 8.10 Hz, H-2$_{phen}$ and H-6$_{phen}$), 5.04 (s, 6H, CH_2), 3.55 (t, 6H, J = 6.90 Hz, NCH_2), 2.25 (t, 6H, J = 6.90 Hz, NCH_2), 2.18 (s, 18H, $N(CH_3)_2$), 1.70–1.65 (m, 6H, CH_2), 1.55–1.51 (m, 6H, CH_2).

1,3,5-*Tris*[(4-(2-(4-methylpiperazin-1-yl)ethyl)iminomethyl)phenoxy)methyl]benzene (**3d**)

Yellow oil (98%); ^{1}H NMR ($CDCl_3$) δ ppm: 8.15 (s, 3H, CH=N), 7.59 (d, 6H, J = 8.10 Hz, H-3$_{phen}$ and H-5$_{phen}$), 7.38 (s, 3H, H$_{benz}$), 6.92 (d, 6H, J = 8.10 Hz, H-2$_{phen}$ and H-6$_{phen}$), 5.02 (s, 6H, CH_2), 3.67 (t, 6H, J = 6.0 Hz, NCH_2), 2.64 (t, 6H, J = 8.40 Hz, NCH_2), 2.23 (s, 24H, NCH_{2pip}), 2.18 (s, 9H, NCH_3).

1,3,5-*Tris*[(4-(3-(4-methylpiperazin-1-yl)propyl)iminomethyl)phenoxy)methyl]benzene (**3e**)

Yellow oil (98%); ^{1}H NMR ($CDCl_3$) δ ppm: 8.20 (s, 3H, CH=N), 7.65 (d, 6H, J = 8.10 Hz, H-3$_{phen}$ and H-5$_{phen}$), 7.45 (s, 3H, H$_{benz}$), 6.98 (d, 6H, J = 8.10 Hz, H-2$_{phen}$ and H-6$_{phen}$), 5.09 (s, 6H, CH_2), 3.61 (t, 6H, J = 6.00 Hz, NCH_2), 2.47 (t, 6H, J = 6.00 Hz, NCH_2), 2.26 (s, 24H, NCH_{2pip}), 2.18 (s, 9H, NCH_3), 1.91–1.86 (m, 6H, CH_2).

1,3,5-*Tris*[(4-(3-(morpholin-1-yl)propyl)iminomethyl)phenoxy)methyl]benzene (**3f**)

Yellow oil (98%); ^{1}H NMR ($CDCl_3$) δ ppm: 8.18 (s, 3H, CH=N), 7.63 (d, 6H, J = 8.10 Hz, H-3$_{phen}$ and H-5$_{phen}$), 7.43 (s, 3H, H$_{benz}$), 6.95 (d, 6H, J = 8.10 Hz, H-2$_{phen}$ and H-6$_{phen}$), 3.67 (t, 12H, J = 4.20 Hz, OCH_2), 3.58 (t, 6H, J = 6.9 Hz, NCH_2), 2.41–2.36 (m, 18H, NCH_2 and NCH_{2morph}), 1.86 (qt, 6H, J = 6.90 Hz, CH_2).

1,3,5-*Tris*[(4-(3-(morpholin-1-yl)propyl)iminomethyl)phenoxy)methyl]benzene (**3f**)

Yellow oil (94%); ^{1}H NMR ($CDCl_3$) δ ppm: 8.18 (s, 3H, CH=N), 7.56 (d, 6H, J = 8.10 Hz, H-3$_{phen}$ and H-5$_{phen}$), 7.12 (d, 6H, J = 8.10 Hz, H-2$_{phen}$ and H-6$_{phen}$), 6.79 (s, 3H, H$_{benz}$), 5.04 (s, 6H, CH_2), 3.65 (t, 12H, J = 4.20 Hz, OCH_2), 3.58 (t, 6H, J = 6.9 Hz, NCH_2), 2.39–2.28 (m, 18H, NCH_2 and NCH_{2morph}), 1.83 (qt, 6H, J = 6.90 Hz, CH_2).

1,3,5-*Tris*[(4-(3-(pyrrolidin-1-yl)propyl)iminomethyl)phenoxy)methyl]benzene (**3g**)

Yellow oil (98%); ^{1}H NMR ($CDCl_3$) δ ppm: 8.20 (s, 3H, CH=N), 7.66 (d, 6H, J = 8.1 Hz, H-3$_{phen}$ and H-5$_{phen}$), 7.44 (s, 3H, H$_{benz}$), 6.97 (d, 6H, J = 8.10 Hz, H-2$_{phen}$ and H-6$_{phen}$), 5.08 (s, 6H, CH_2), 3.62 (t, 6H, J = 6.60 Hz, NCH_2), 2.54–2.47 (m, 18H, NCH_2 and $NCH_{2pyrrol}$), 1.93 (t, 6H, J = 6.60 Hz, CH_2), 1.79–1.74 (m, 12H, $CH_{2pyrrol}$).

1,3,5-*Tris*[(4-(3-(piperidin-1-yl)propyl)iminomethyl)phenoxy)methyl]benzene (**3h**)

Yellow oil (99%); ^{1}H NMR ($CDCl_3$) δ ppm: 8.19 (s, 3H, CH=N), 7.65 (d, 6H, J = 8.10 Hz, H-3$_{phen}$ and H-5$_{phen}$), 6.97 (d, 6H, J = 8.10 Hz, H-2$_{phen}$ and H-6$_{phen}$), 7.44 (s, 3H, H$_{benz}$), 5.08 (s, 6H, CH_2), 3.63 (t, 6H, J = 6.90 Hz, NCH_2), 2.40–2.34 (m, 18H, NCH_2 and NCH_{2pip}), 1.88 (t, 6H, J = 6.90 Hz, CH_2), 1.62–1.54 (m, 12H, CH_{2pip}), 1.45–1.42 (m, 6H, CH_{2pip}).

1,3,5-*Tris*{[4-((quinolin-3-yl)iminomethyl)phenoxy]methyl}benzene (**3i**)

Pale-yellow oil (98%); ^{1}H NMR ($CDCl_3$) δ ppm: 8.91 (s, 3H, CH=N), 8.49 (d, 3H, J = 2.70 Hz, H-2$_{quinol}$), 8.24–8.19 (m, 3H, H-8$_{quinol}$), 8.02–7.99 (m, 3H, H-5$_{quinol}$), 7.97 (d, 3H, J = 2.70 Hz, H-4$_{quinol}$), 7.61 (d, 6H, J = 7.80 Hz, H-3$_{phen}$ and H-5$_{phen}$), 7.50–7.39 (m, 6H, H-6$_{quinol}$ and H-7$_{quinol}$), 7.23 (d, 6H, J = 7.80 Hz, H-2$_{phen}$ and H-6$_{phen}$), 7.12 (s, 3H, H$_{benz}$), 5.12 (s, 6H, CH_2).

1,3,5-*Tris*[(4-(pyridin-2-ylmethyliminomethyl)phenoxy)methyl]benzene (**3j**)

Pale-yellow oil (93%); ^{1}H NMR ($CDCl_3$) δ ppm: 8.53 (d, 3H, J = 6.90 Hz, H-6$_{pyrid}$), 8.36 (s, 3H, CH=N), 7.73 (d, 6H, J = 8.10 Hz, H-3$_{phen}$ and H-5$_{phen}$), 7.71–7.58 (m, 3H, H-4$_{pyrid}$), 7.44–7.38 (m, 6H, H-3$_{pyrid}$ and H-5$_{pyrid}$), 7.10 (s, 3H, H$_{benz}$), 6.99 (t, 6H, J = 8.10 Hz, H-2$_{phen}$, H-6$_{phen}$), 5.07 (s, 6H, CH_2), 4.90 (s, 6H, NCH_2).

1,3,5-*Tris*[(4-(pyridin-2-ylethyliminomethyl)phenoxy)methyl]benzene (**3k**)

Yellow oil (97%); ^{1}H NMR ($CDCl_3$) δ ppm: 8.52 (d, 3H, J = 5.90 Hz, H-6$_{pyrid}$), 8.13 (s, 3H, CH=N), 7.63 (d, 6H, J = 8.10 Hz, H-3$_{phen}$ and H-5$_{phen}$), 7.71–7.58 (m, 3H, H-4$_{pyrid}$),

7.45 (s, 3H, H_{benz}), 7.22–7.11 (m, 6H, H-3_{pyrid} and H-5_{pyrid}), 6.99 (t, 6H, *J* = 8.10 Hz, H-2_{phen}, H-6_{phen}), 5.08 (t, 6H, *J* = 7.20 Hz, CH_2), 3.98 (s, 6H, NCH_2), 3.17 (t, 6H, *J* = 7.20 Hz, CH_2Pyrid).

1,3,5-*Tris*[(4-(pyridin-2-ylpropyliminomethyl)phenoxy)methyl]benzene (**3l**)

Yellow oil (97%); ^{1}H NMR ($CDCl_3$) δ ppm: 8.48 (d, 3H, *J* = 5.80 Hz, H-6_{pyrid}), 8.15 (s, 3H, CH=N), 7.63 (d, 6H, *J* = 8.10 Hz, H-3_{phen} and H-5_{phen}), 7.58–7.50 (m, 3H, H-4_{pyrid}), 7.42 (s, 3H, H_{benz}), 7.12–7.03 (m, 6H, H-3_{pyrid} and H-5_{pyrid}), 6.94 (t, 6H, *J* = 8.10 Hz, H-2_{phen}, H-6_{phen}), 5.05 (t, 6H, *J* = 7.20 Hz, CH_2), 3.62 (t, 6H, *J* = 6.60 Hz, NCH_2), 2.82 (t, 6H, *J* = 6.60 Hz, CH_2Pyrid), 2.12 (qt, 6H, *J* = 6.60 Hz, CH_2).

1,3,5-*Tris*[(4-(pyridin-3-ylmethyliminomethyl)phenoxy)methyl]benzene (**3m**)

Pale-yellow oil (98%); ^{1}H NMR ($CDCl_3$) δ ppm: 8.60–8.46 (m, 6H, H-2_{pyrid} and H-6_{pyrid}), 8.34 (s, 3H, CH=N), 7.67–7.62 (m, 9H, H-3_{phen}, H-5_{phen} and H-4_{pyrid}), 7.46 (s, 3H, H_{benz}), 7.24 (m, 3H, H-5_{pyrid}), 6.94 (t, 6H, *J* = 8.10 Hz, H-2_{phen}, H-6_{phen}), 5.11 (s, 6H, CH_2), 4.76 (s, 6H, NCH_2).

1,3,5-*Tris*[(4-(pyridin-3-ylethyliminomethyl)phenoxy)methyl]benzene (**3n**)

Yellow oil (97%); ^{1}H NMR ($CDCl_3$) δ ppm: 8.40–8.31 (m, 6H, H-2_{pyrid} and H-6_{pyrid}), 8.06 (s, 3H, CH=N), 7.52 (d, 6H, *J* = 7.80 Hz, H-3_{phen} and H-5_{phen}), 7.43–7.7.38 (m, 3H, H-4_{pyrid}), 6.62 (s, 3H, H_{benz}), 7.447–6.88 (m, 9H, H-2_{phen}, H-6_{phen} and H-5_{pyrid}), 5.20 (s, 6H, CH_2), 3.79 (t, 6H, *J* = 7.20 Hz, NCH_2), 2.98 (t, 6H, *J* = 7.20 Hz, CH_2Pyrid).

1,3,5-*Tris*[(4-(pyridin-3-ylpropyliminomethyl)phenoxy)methyl]benzene (**3o**)

Yellow oil (97%); ^{1}H NMR ($CDCl_3$) δ ppm: 8.45 (d, 3H, *J* = 2.20 Hz, H-2_{pyrid}), 8.43 (dd, 3H, *J* = 4.80 and 1.60 Hz, H-6_{pyrid}), 8.20 (s, 3H, CH=N), 7.70 (d, 6H, *J* = 8.10 Hz, H-3_{phen}, and H-5_{phen}), 7.42 (s, 3H, H_{benz}), 7.26–7.15 (m, 6H, H-4_{pyrid} and H-5_{pyrid}), 7.02 (d, 6H, *J* = 8.10 Hz, H-2_{phen} and H-6_{phen}), 5.11 (s, 6H, CH_2), 3.61 (t, 6H, *J* = 6.60 Hz, NCH_2), 2.73 (t, 6H, *J* = 6.60 Hz, CH_2Pyrid), 2.04 (qt, 6H, *J* = 6.60 Hz, CH_2).

1,3,5-*Tris*[(4-(pyridin-4-ylmethyliminomethyl)phenoxy)methy]benzene (**3p**)

Pale-yellow oil (98%); ^{1}H NMR ($CDCl_3$) δ ppm: 8.52 (d, 6H, *J* = 5.40 Hz, H-2_{pyrid} and H-6_{pyrid}), 8.30 (s, 3H, CH=N), 7.72 (d, 6H, *J* = 8.10 Hz, H-3_{phen} and H-5_{phen}), 7.46 (s, 3H, H_{benz}), 7.26–7.24 (m, 6H, H-4_{pyrid} and H-5_{pyrid}), 7.00 (d, 6H, *J* = 8.10 Hz, H-2_{phen} and H-6_{phen}), 5.10 (s, 6H, CH_2), 4.73 (s, 6H, NCH_2).

1,3,5-*Tris*[(4-(pyridin-4-ylethyliminomethyl)phenoxy)methyl]benzene (**3q**)

Yellow oil (97%); ^{1}H NMR ($CDCl_3$) δ ppm: 8.51–8.50 (m, 6H, H-2_{pyrid} and H-6_{pyrid}), 8.10 (s, 3H, CH=N), 7.65 (d, 6H, *J* = 8.20 Hz, H-3_{phen} and H-5_{phen}), 7.50 (s, 3H, H_{benz}), 7.26–7.20 (m, 6H, H-3_{pyrid} and H-5_{pyrid}), 7.04 (d, 6H, *J* = 8.20 Hz, H-2_{phen} and H-6_{phen}), 5.14 (s, 6H, CH_2), 3.85 (t, 6H, *J* = 7.20 Hz, NCH_2), 3.02 (t, 6H, *J* = 7.20 Hz, CH_2Pyrid).

1,3,5-*Tris*[(4-(pyridin-4-ylpropyliminomethyl)phenoxy)methyl]benzene (**3r**)

Yellow oil (98%); ^{1}H NMR ($CDCl_3$) δ ppm: 8.47 (d, 6H, *J* = 5.40 Hz, H-2_{pyrid} and H-6_{pyrid}), 8.18 (s, 3H, CH=N), 7.66 (d, 6H, *J* = 7.80 Hz, H-3_{phen} and H-5_{phen}), 7.47 (s, 3H, H_{benz}), 7.14–7.11 (m, 6H, H-3_{pyrid} and H-5_{pyrid}), 7.01 (d, 6H, *J* = 8.20 Hz, H-2_{phen} and H-6_{phen}), 5.10 (s, 6H, CH_2), 3.58 (t, 6H, *J* = 7.20 Hz, NCH_2), 2.69 (t, 6H, *J* = 7.20 Hz, CH_2Pyrid), 2.02 (qt, 6H, *J* = 7.20 Hz, CH_2).

3.1.4. General Procedure for the Synthesis of 1,3,5-*Tris*[(4-(Substituted-Aminomethyl) Phenoxy)Methyl]Benzenes **4a–r**

Compound **3a–r** (0.4 mmol) was dissolved in methanol (10 mL), and sodium borohydride (3.2 mmol, 8 eq.) was added gradually at 0 °C. The resulting mixture was stirred at room temperature for 2 h. Subsequently, the solvent was removed under reduced pressure, and the residue obtained was cooled, triturated in water, and then extracted with dichloromethane (40 mL). After separating, the organic layer was dried with sodium sulfate, filtered, and evaporated to dryness. The resulting residue was subjected to purification via column chromatography on silica gel, using dichloromethane/methanol (90/10, *v*/*v*) as the eluent, yielding the pure products **4a–r**.

1,3,5-*Tris*[(4-(2-dimethylaminoethyl)aminomethyl)phenoxy)methyl]benzene (**4a**)

Yellow oil (90%); ^{1}H NMR ($CDCl_3$) δ ppm: 3.88 (s, 6H, CH_2),7.26 (d, 6H, J = 8.10 Hz, H-3_{phen} and H-5_{phen}), 7.92 (d, 6H, J = 8.10 Hz, H-2_{phen} and H-6_{phen}), 5.07 (s, 6H, OCH_2), 3.74 (t, 6H, J = 6.90 Hz, NCH_2), 2.68 (t, 6H, J = 6.90 Hz, NCH_2), 2.44 (t, 6H, J = 6.90 Hz, NCH_2), 2.19 (s, 18H, $N(CH_3)_2$); ^{13}C NMR ($CDCl_3$) δ ppm: 159.07 (C-4_{phenyl}), 139.32 (Cq_{benz}), 134.27 (C-1_{phenyl}), 130.77 (C-3_{phen} and C-5_{phen}), 127.25 (CH_{benz}), 116.10 (C-2_{phen} and C-6_{phen}), 71.11 (OCH_2), 60.40 (NCH_2), 54.80 (NCH_2), 44.84 (NCH_2), 46.88 ($N(CH_3)_2$), ESI-MS m/z $[M+H]^+$ calculated for $C_{42}H_{61}N_6$: 697.4902, found: 697.4852.

1,3,5-*Tris*[(4-(3-dimethylaminopropyl)aminomethyl)phenoxy)methyl]benzene (**4b**)

Yellow oil (81%); ^{1}H NMR ($CDCl_3$) δ ppm: 7.40 (s, 3H, H_{benz}), 7.20 (d, 6H, J = 8.10 Hz, H-3_{phen} and H-5_{phen}), 6.97 (d, 6H, J = 8.10 Hz, H-2_{phen} and H-6_{phen}), 5.80 (s, 6H, OCH_2), 3.70 (s, 6H, NCH_2), 2.64 (t, 6H, J = 7.10 Hz, NCH_2), 2.29 (t, 6H, J = 7.10 Hz, NCH_2), 2.19 (s, 18H, $N(CH_3)_2$), 1.66 (qt, 6H, J = 7.10 Hz, CH_2); ^{13}C NMR ($CDCl_3$) δ ppm: 159.6 (C-4_{phenyl}), 139.33 (Cq_{benz}), 134.44 (C-1_{phenyl}), 130.26 (C-3_{phen} and C-5_{phen}), 127.22 (CH_{benz}), 116.26 (C-2_{phen} and C-6_{phen}), 71.11 (OCH_2), 59.42 (NCH_2), 54.80 (NCH_2), 49.17 (NCH_2) 46.91 ($N(CH_3)_2$), 29.40 (CH_2). ESI-MS m/z $[M+H]^+$ calculated for $C_{45}H_{68}N_6$: 739.54, found: 739.52.

1,3,5-*Tris*[(4-(4-dimethylaminobutyl)aminomethyl)phenoxy)methyl]benzene (**4c**)

Yellow oil (83%); ^{1}H NMR ($CDCl_3$) δ ppm: 7.42 (s, 3H, H_{benz}), 7.23 (d, 6H, J = 7.90 Hz, H-3_{phen} and H-5_{phen}), 6.92 (d, 6H, J = 7.90 Hz, H-2_{phen} and H-6_{phen}), 5.02 (s, 6H, OCH_2), 3.70 (s, 6H, NCH_2), 2.61 (t, 6H, J = 6.90 Hz, NCH_2), 2.23 (t, 6H, J = 6.90 Hz, NCH_2), 2.16 (s, 18H, $N(CH_3)_2$), 1.50–1.48 (m, 12H, CH_2); ^{13}C NMR ($CDCl_3$) δ ppm: 159.11 (C-4_{phenyl}), 139.29 (Cq_{benz}), 134.14 (C-1_{phenyl}), 130.76 (C-3_{phen} and C-5_{phen}), 127.83 (CH_{benz}), 116.12 (C-2_{phen} and C-6_{phen}), 71.03 (OCH_2), 60.99 (NCH_2), 54.65 (NCH_2), 50.54 (NCH_2), 46.76 ($N(CH_3)_2$), 29.25 (CH_2), 26.89 (CH_2). ESI-MS m/z $[M+H]^+$ calculated for $C_{48}H_{73}N_6$: 781.12, found: 781.5812.

1,3,5-*Tris*[(4-(2-(4-methylpiperazin-1-yl)ethyl)aminomethyl)phenoxy)methyl]benzene (**4d**)

Yellow oil (64%); ^{1}H NMR ($CDCl_3$) δ ppm: 7.39 (s, 3H, H_{benz}), 7.18 (d, 6H, J = 8.10 Hz, H-3_{phen} and H-5_{phen}), 6.87 (d, 6H, J = 8.10 Hz, H-2_{phen} and H-6_{phen}), 4.99 (s, 6H, OCH_2), 3.66 (s, 6H, NCH_2), 2.62 (t, 6H, J = 6.90 Hz, NCH_2), 2.46 (t, 6H, J = 6.90 Hz, NCH_2), 2.48–2.35 (m, 24H, $NCH_{2piperazine}$), 2.27 (s, 9H, NCH_3); ^{13}C NMR ($CDCl_3$) δ ppm: 159.06 (C-4_{phenyl}), 139.29 (Cq_{benz}), 134.30 (C-1_{phenyl}), 130.66 (C-3_{phen} and C-5_{phen}), 127.19 (CH_{benz}), 116.20 (C-2_{phen} and C-6_{phen}), 71.07 (OCH_2), 59.001 (NCH_2), 56.44 ($NCH_{2piperazine}$), 54.45 ($NCH_{2piperazine}$), 47.04 (NCH_3), 42.83 (CH_2). ESI-MS m/z $[M+H]^+$ calculated for $C_{51}H_{76}N_9$: 861.60, found: 861.61.

1,3,5-*Tris*[(4-(3-(4-methylpiperazin-1-yl)propyl)aminomethyl)phenoxy)methyl]benzene (**4e**)

Yellow oil (72%); ^{1}H NMR ($CDCl_3$) δ ppm: 7.43 (s, 3H, H_{benz}), 7.20 (d, 6H, J = 8.10 Hz, H-3_{phen} and H-5_{phen}), 6.90 (d, 6H, J = 8.10 Hz, H-2_{phen} and H-6_{phen}), 5.03 (s, 6H, OCH_2), 3.68 (s, 6H, NCH_2), 2.64 (t, 6H, J = 7.10 Hz, NCH_2), 2.37 (t, 6H, J = 7.10 Hz, NCH_2), 2.41–2.34 (m, 24H, $NCH_{2piperazine}$), 2.23 (s, 9H, NCH_3), 1.67 (qt, 6H, J = 7.10 Hz, CH_2); ^{13}C NMR ($CDCl_3$) δ ppm: 159.03 (C-4_{phenyl}), 139.31 (Cq_{benz}), 134.25 (C-1_{phenyl}), 130.67 (C-3_{phen} and C-5_{phen}), 127.24 (CH_{benz}), 116.11 (C-2_{phen} and C-6_{phen}), 71.11 (OCH_2), 58.27 (NCH_2), 56.44 ($NCH_{2piperazine}$), 54.70 (CH2), 54.53 ($NCH_{2piperazine}$), 49.35 (NCH_2), 42.77 (NCH_3), 28.20 (CH_2). ESI-MS m/z $[M+H]^+$ calculated for $C_{54}H_{82}N_9$: 903.65, found: 903.26.

1,3,5-*Tris*[(4-(3-(morpholin-1-yl)propyl)aminomethyl)phenoxy)methyl]benzene (**4f**)

Yellow oil (90%); ^{1}H NMR ($CDCl_3$) δ ppm: 7.42 (s, 3H, H_{benz}), 7.20 (d, 6H, J = 8.10 Hz, H-3_{phen} and H-5_{phen}), 6.91 (d, 6H, J = 8.10 Hz, H-2_{phen} and H-6_{phen}), 5.02 (s, 6H, OCH_2), 3.68–3.64 (m, 18H, NCH_2 and OCH_2), 2.64 (t, 6H, J = 6.90 Hz, NCH_2), 2.38 (t, 12H, J = 4.65 Hz, $NCH_{2\ morpholine}$), 2.33 (t, 6H, J = 6.90 Hz, NCH_2), 1.66 (qt, 6H, J = 6.90 Hz, CH_2); ^{13}C NMR ($CDCl_3$) δ ppm: 157.69 (C-4_{phenyl}), 137.92 (Cq_{benz}), 132.91 (C-1_{phenyl}), 129.24 (C-3_{phen} and C-5_{phen}), 125.86 (CH_{benz}), 114.73 (C-2_{phen} and C-6_{phen}), 69.70 (OCH_2), 66.92 ($OCH_{2morpholine}$), 57.35 (NCH_2), 53.75 ($NCH_{2morpholine}$), 53.36 (NCH_2), 47.85 (NCH_2), 26.58 (CH_2). ESI-MS m/z $[M+H]^+$ calculated for $C_{51}H_{73}N_6O_3$: 866.15, found: 866.56.

1,3,5-*Tris*[(4-(3-(pyrrolidin-1-yl)propyl)aminomethyl)phenoxy)methyl]benzene (**4g**)

Yellow oil (91%); ^{1}H NMR ($CDCl_3$) δ ppm: 7.43 (s, 3H, H_{benz}), 7.21 (d, 6H, J = 8.10 Hz, H-3_{phen} and H-5_{phen}), 6.90 (d, 6H, J = 8.10 Hz, H-2_{phen} and H-6_{phen}), 5.04 (s, 6H, OCH_2), 3.70 (s, 6H, NCH_2), 5.50 (t, 6H, J = 6.90 Hz, NCH_2), 2.48–2.45 (m, 18H, NCH_2 and

$NCH_{2pyrrolidine}$), 1.76–1.71 (m, 18H, CH_2 and $CH_{2pyrrolidine}$); ^{13}C NMR ($CDCl_3$) δ ppm: 159.09 (C-4_{phenyl}), 139.33 (Cq_{benz}), 134.42 (C-1_{phenyl}), 130.64 (C-3_{phen} and C-5_{phen}), 127.21 (CH_{benz}), 116.12 (C-2_{phen} and C-6_{phen}), 71.12 (OCH_2), 56.12 (NCH_2), 55.60 ($NCH_{2pyrrolidine}$), 54.72 (NCH_2), 49.34 (NCH_2), 30.57 (CH_2), 24.79 ($CH_{2pyrrolidine}$). ESI-MS m/z $[M+H]^+$ calculated for $C_{51}H_{73}N_6$: 817.57, found: 817.5722.

1,3,5-*Tris*[(4-(3-(piperidin-1-yl)propyl)aminomethyl)phenoxy)methyl]benzene (**4h**)

Yellow oil (99%); ^1H NMR ($CDCl_3$) δ ppm: 7.40 (s, 3H, H_{benz}), 7.16 (d, 6H, J = 8.10 Hz, H-3_{phen} and H-5_{phen}), 6.87 (d, 6H, J = 8.10 Hz, H-2_{phen} and H-6_{phen}), 4.99 (s, 6H, OCH_2), 3.66 (s, 6H, NCH_2), 2.66 (t, 6H, J = 6.90 Hz, NCH_2), 2.33–2.26 (m, 18H, NCH_2 and $NCH_{2piperidine}$), 1.65 (qt, 6H, J = 6.90 Hz, CH_2), 1.60–1.50 (m, 12H, $CH_{2piperidine}$), 1.38–1.36 (m, 6H, $CH_{2piperidine}$); ^{13}C NMR ($CDCl_3$) δ ppm: 159.05 (C-4_{phenyl}), 139.30 (Cq_{benz}), 134.31 (C-1_{phenyl}), 130.64 (C-3_{phen} and C-5_{phen}), 127.18 (CH_{benz}), 116.00 (C-2_{phen} and C-6_{phen}), 71.08 (OCH_2), 59.80 (NCH_2), 55.99 ($NCH_{2\ piperidine}$), 54.65 (NCH_2), 49.47 (CH_2), 28.25 (CH_2), 27.30 ($CH_{2piperidine}$), 25.80 ($CH_{2piperidine}$). ESI-MS m/z $[M+H]^+$ calculated for $C_{54}H_{79}N_6$: 859.61, found: 859.6276.

1,3,5-*Tris*[(4-((quinolin-3-yl)aminomethyl)phenoxy)methyl]benzene (**4i**)

Pale-yellow crystals (95%); M.p. = 135 °C; ^1H NMR ($CDCl_3$) δ ppm: 8.50 (d, 3H, J = 2.70 Hz, H-2_{quinol}), 7.96 (s, 3H, H_{benz}), 7.69 (dd, 3H, J = 6.90 and 3.60 Hz, H-8_{quinol}), 7.59 (dd, 3H, J = 6.90 and 3.60 Hz, H-5_{quinol}), 7.44–7.39 (m, 6H, H-6_{quinol} and H-7_{quinol}), 7.29 (d, 6H, J = 7.80 Hz, H-3_{phen} and H-5_{phen}), 6.98 (d, 6H, J = 7.80 Hz, H-2_{phen} and H-6_{phen}), 7.03 (d, 3H, J = 2.70 Hz, H-4_{quinol}), 5.10 (s, 6H, OCH_2), 4.38 (s, 6H, NCH_2); ^{13}C NMR ($CDCl_3$) δ ppm: 158.11 (C-4_{phenyl}), 143.50 (C-$8a_{quinol}$), 141.51 (Cq_{benz}), 137.87 (C-1_{phenyl}), 134.93 (C-$4a_{quinol}$), 130.76 (C-2_{quinol}), 130.61 (C-3_{phen} and C-5_{phen}), 130.35 (C-4_{quinol}), 129.03 (C-3_{quinol}),129.02 (C-2_{phen} and C-6_{phen}), 129.00 (C-8_{quinol}), 128.33 (CH_{benz}), 127.37 (C-6_{quinol}), 126.40 (C-7_{quinol}), 110.39 (C-5_{quinol}), 69.75 (OCH_2), 47.31 (NCH_2). ESI-MS m/z $[M+H]^+$ calculated for $C_{57}H_{49}N_6$: 865.38, found: 865.38.

1,3,5-*Tris*[(4-(pyridin-2-ylmethylaminomethyl)phenoxy)methyl]benzene (**4j**)

Yellow oil (92%); ^1H NMR ($CDCl_3$) δ ppm: 8.57–8.55 (m, 3H, H-6_{pyrid}), 7.67–7.60 (m, 3H, H-4_{pyrid}), 7.48 (s, 3H, H_{benz}), 7.33–7.25 (m, 9H, H-3_{phen}, H-5_{phen}, and H-3_{pyrid}), 7.18–7.15 (m, 3H, H-5_{pyrid}), (d, 6H, J = 7.80 Hz, H-6_{phen} and H-2_{phen}), 5.08 (s, 6H, OCH_2), 3.92 (s, 6H, NCH_2), 3.79 (s, 6H, NCH_2); ^{13}C NMR ($CDCl_3$) δ ppm: 161.22 (C-4_{phenyl}), 159.00 (C-2_{pyrid}), 150.66 (C-6_{pyrid}), 139.37 (Cq_{benz}), 137.84 (C-4_{pyrid}), 134.13 (C-1_{phenyl}), 130.28 (C-3_{phen} and C-5_{phen}), 127.26 (CH_{benz}), 116.19 (C-2_{phen} and C-6_{phen}), 123.28 (C-5_{pyrid}), 123.73 (C-3_{pyrid}), 71.16 (OCH_2), 55.83 (NCH_2), 54.28 (CH_2). ESI-MS m/z $[M+H]^+$ calculated for $C_{48}H_{49}N_6$: 757.38, found: 758.39.

1,3,5-*Tris*[(4-(pyridin-2-ylethylaminomethyl)phenoxy)methyl]benzene (**4k**)

Yellow oil (95%); ^1H NMR ($CDCl_3$) δ ppm: 8.52–8.50 (m, 3H, H-6_{pyrid}), 7.57–7.56 (m, 3H, H-4_{pyrid}), 7.45 (s, 3H, H_{benz}), 7.23–7.14 (m, 12H, H-3_{phen}, H-5_{phen}, H-$3_{pyrid,}$ and H-5_{pyrid}), 6.93–6.90 (d, 6H, J = 7.80 Hz, H-6_{phen} and H-2_{phen}), 3.76 (s, 6H, NCH_2), 3.77 (s, 6H, CH_2), 3.02–3.00 (m, 12H, NCH_2 and CH_2Pyrid); ^{13}C NMR ($CDCl_3$) δ ppm: 159.12 (C-2_{pyrid}), 159.13 (C-4_{phenyl}), 150.67 (C-6_{pyrid}), 139.34 (Cq_{benz}), 137.16 (C-4_{pyrid}), 130.75 (C-1_{phenyl}), 130.75 (C-3_{phen} and C-5_{phen}), 127.25 (C-3_{pyrid}), 124.63 (C-5_{pyrid}), 122.63 (CH_{benz}), 116.15 (C-2_{phen} and C-6_{phen}), 71.12 (OCH_2), 54.54 (NCH_2), 50.07 (NCH_2), 39.68 (CH_2). ESI-MS m/z $[M+H]^+$ calculated for $C_{51}H_{55}N_6$: 799.43, found: 799.4317.

1,3,5-*Tris*[(4-(pyridin-2-ylpropylaminomethyl)phenoxy)methyl]benzene (**4l**)

Yellow oil (98%); ^1H NMR ($CDCl_3$) δ ppm: 8.50–8.48 (m, 3H, H-6_{pyrid}), 7.55–7.48 (m, 3H, H-4_{pyrid}), 7.45 (s, 3H, H_{benz}), 7.21 (d, 6H, J = 8.10 Hz, H-3_{phen} and H-5_{phen}), 7.11–7.01 (m, 6H, H-5_{pyrid}, and H-3_{pyrid}), 6.91 (m, 6H, J = 8.10, H-6_{phen} and H-2_{phen}), 5.05 (s, 6H, OCH_2), 3.71 (s, 6H, NCH_2), 2.81 (t, 6H, J = 6.90 Hz, NCH_2), 2.66 (t, 6H, J = 6.90 Hz, CH_2Pyrid), 1.92 (qt, J = 6.90 Hz, CH_2); ^{13}C NMR ($CDCl_3$) δ ppm: 159.07 (C-2_{pyrid}), 159.02 (C-4_{phenyl}), 150.57 (C-6_{pyrid}), 139.36 (Cq_{benz}), 139.36 (C-4_{pyrid}), 134.51 (C-1_{phenyl}), 130.37 (C-3_{phen} and C-5_{phen}), 127.25 (C-3_{pyrid}), 124.11 (C-5_{pyrid}), 122.35 (CH_{benz}), 116.12 (C-2_{phen} and C-6_{phen}), 71.14 (OCH_2), 54.66 (NCH_2), 50.08 (NCH_2), 37.26 (CH_2), 31.37 (CH_2). ESI-MS m/z $[M+H]^+$ calculated for $C_{54}H_{61}N_6$: 841.47, found: 841.48.

1,3,5-*Tris*[(4-(pyridin-3-ylmethylaminomethyl)phenoxyl)methyl]benzene (**4m**)

Pale-yellow oil (96%); ^{1}H NMR ($CDCl_3$) δ ppm: 8.57–8.48 (m, 6H, H-6_{pyrid} and H-2_{pyrid}), 7.69 (d, 3H, J = 7.80 Hz, H-4_{pyrid}), 7.45 (s, 3H, H_{benz}), 7.25–7.23 (m, 3H, H-5_{pyrid}), 7.23 (d, 6H, J = 8.10 Hz, H-3_{phen} and H-5_{phen}), 6.93 (d, 6H, J = 8.10 Hz, H-6_{phen} and H-2_{phen}), 5.05 (s, 6H, OCH_2), 3.77 (s, 6H, NCH_2), 3.72 (s, 6H, CH_2); ^{13}C NMR ($CDCl_3$) δ ppm: 159.22 (C-4_{phenyl}), 151.10 (C-2_{pyrid}), 149.80 (C-6_{pyrid}), 139.32 (C-3_{pyrid}), 137.29 (C-4_{pyrid}), 137.02 (Cq_{benz}), 133.89 (C-1_{phenyl}), 130.76 (C-3_{phen} and C-5_{phen}), 127.31 (CH_{benz}), 124.78 (C-5_{pyrid}), 116.21 (C-2_{phen} and C-6_{phen}), 72.15 (OCH_2), 53.94 (NCH_2), 51.70 (CH_2). ESI-MS m/z $[M+H]^+$ calculated for $C_{48}H_{49}N_6$: 755.36, found: 755.3922

1,3,5-*Tris*[(4-(pyridin-3-ylethylaminomethyl)phenoxy)methyl]benzene (**4n**)

Yellow oil (94%); ^{1}H NMR ($CDCl_3$) δ ppm: 8.45–8.43 (m, 6H, H-6_{pyrid} and H-2_{pyrid}), 7.47–7.44 (m, 6H, H-4_{pyrid} and H-5_{pyrid}), 7.43 (s, 3H, H_{benz}), 7.17 (d, 6H, J = 7.80 Hz, H-3_{phen} and H-5_{phen}), 6.91 (d, 6H, J = 7.80 Hz, H-6_{phen} and H-2_{phen}), 5.03 (s, 6H, OCH_2), 3.72 (s, 6H, NCH_2), 2.86–2.77 (m, 12H, NCH_2 and CH_2Pyrid); ^{13}C NMR ($CDCl_3$) δ ppm: 159.15 (C-4_{phenyl}), 151.47 (C-2_{pyrid}), 148.97 (C-6_{pyrid}), 139.00 (C-3_{pyrid}), 137.55 (C-4_{pyrid}), 137.62 (Cq_{benz}), 134.04 (C-1_{phenyl}), 130.68 (C-3_{phen} and C-5_{phen}), 127.29 (CH_{benz}), 124.74 (C-5_{pyrid}), 116.16 (C-2_{phen} and C-6_{phen}), 71.09 (OCH_2), 54.54 (NCH_2), 51.36 (NCH_2), 34.83 (CH_2). ESI-MS m/z $[M+H]^+$ calculated for $C_{51}H_{55}N_6$: 799.43, found: 799.4386.

1,3,5-*Tris*[(4-(pyridin-3-ylpropylaminomethyl)phenoxy)methyl]benzene (**4o**)

Yellow oil (98%); ^{1}H NMR ($CDCl_3$) δ ppm: 8.44–8.41 (m, 6H, H-6_{pyrid} and H-2_{pyrid}), 7.47–7.44 (m, 6H, H-4_{pyrid} and H-5_{pyrid}), 7.20 (s, 3H, H_{benz}), 7.18 (d, 6H, J = 8.10 Hz, H-3_{phen} and H-5_{phen}), 7.09 (d, 6H, J = 8.10 Hz, H-6_{phen} and H-2_{phen}), 5.02 (s, 6H, OCH_2), 3.67 (s, 6H, NCH_2), 2.67–2.60 (m, 12H, NCH_2 and CH_2Pyrid), 1.77 (qt, 6H, J = 7.20 Hz, CH_2);

^{13}C NMR ($CDCl_3$) δ ppm: 159.02 (C-4_{phenyl}), 151.23 (C-2_{pyrid}), 148.60 (C-6_{pyrid}), 141.26 (Cq_{benz}), 139.27 (C-1_{phenyl}), 138.76 (C-3_{pyrid}), 137.24 (C-4_{pyrid}), 130.69 (C-3_{phen} and C-5_{phen}), 127.27 (CH_{benz}), 124.66 (C-5_{pyrid}), 116.12 (C-2_{phen} and C-6_{phen}), 71.08 (OCH_2), 54.73 (NCH_2), 49.86 (NCH_2), 32.01 (CH_2), 31.66 (CH_2). ESI-MS m/z $[M+H]^+$ calculated for $C_{54}H_{61}N_6$: 841.47, found: 841.4788.

1,3,5-*Tris*[(4-(pyridin-4-ylmethylaminomethyl)phenoxy)methyl]benzene (**4p**)

Yellow oil (79%); ^{1}H NMR ($CDCl_3$) δ ppm: 8.57 (d, 6H, J = 6.00 Hz, H-2_{pyrid} and H-6_{pyrid}), 7.48 (s, 3H, H_{benz}), 7.30–7.23 (m, 12H, H-3_{pyrid}, H-5_{pyrid}, H-3_{phen}, and H-5_{phen}), 6.96 (d, 6H, J = 8.10 Hz, H-6_{phen} and H-2_{phen}), 5.02 (s, 6H, OCH_2), 3.82 (s, 6H, NCH_2), 3.73 (s, 6H, NCH_2); ^{13}C NMR ($CDCl_3$) δ ppm: 159.20 (C-4_{phenyl}), 151.12 (C-2_{pyrid} and C-6_{pyrid}), 139.36 (C-4_{pyrid}), 133.78 (Cq_{benz}), 130.32 (C-3_{phen} and C-5_{phen}), 138.84 (C-1_{phenyl}), 124.42 (CH_{benz}), 127.39 (C-3_{pyrid} and C-5_{pyrid}), 116.22 (C-2_{phen} and C-6_{phen}), 71.14 (OCH_2), 53.96 (NCH_2), 53.10 (NCH_2). ESI-MS m/z $[M+H]^+$ calculated for $C_{48}H_{49}N_6$: 757.38, found 757.3850.

1,3,5-*Tris*[(4-(pyridin-4-ylethylaminomethyl)phenoxy)methyl]benzene (**4q**)

Yellow oil (96%); ^{1}H NMR ($CDCl_3$) δ ppm: 8.48–8.47 (m, 6H, H-2_{pyrid} and H-6_{pyrid}), 7.47 (s, 3H, H_{benz}), 7.41 (d, 6H, J = 8.10 Hz, H-3_{phen} and H-5_{phen}), 7.20–7.13 (m, 12H, H-3_{pyrid}, H-5_{pyrid}, H-6_{phen} and H-2_{phen}), 5.08 (s, 6H, OCH_2), 3.73 (s, 6H, NCH_2), 2.90 (t, 6H, J = 6.90 Hz, CH_2), 2.80 (t, 6H, J = 6.90 Hz, CH_2); ^{13}C NMR ($CDCl_3$) δ ppm: 159.20 (C-4_{phenyl}), 151.16 (C-2_{pyrid} and C-6_{pyrid}), 139.54 (C-4_{pyrid}), 133.78 (Cq_{benz}), 138.84 (C-1_{phenyl}), 130.72 (C-3_{phen} and C-5_{phen}), 124.42 (CH_{benz}), 127.39 (C-3_{pyrid} and C-5_{pyrid}), 116.22 (C-2_{phen} and C-6_{phen}), 71.14 (OCH_2), 54.54 (NCH_2), 50.55 (NCH_2), 37.13 (CH_2). ESI-MS m/z $[M+H]^+$ calculated for $C_{51}H_{55}N_6$: 799.43, found: 799.4318.

1,3,5-*Tris*[(4-(pyridin-4-ylpropylaminomethyl)phenoxy)methyl]benzene (**4r**)

Yellow oil (99%); ^{1}H NMR ($CDCl_3$) δ ppm: 8.45–8.43 (m, 6H, H-2_{pyrid} and H-6_{pyrid}), 7.45 (s, 3H, H_{benz}), 7.18–7.08 (m, 6H, H-3_{pyrid} and H-5_{pyrid}), 7.05 (d, 6H, J = 8.10 Hz, H-3_{phen} and H-5_{phen}), 6.93 (d, 6H, H-6_{phen} and H-2_{phen}), 5.04 (s, 6H, OCH_2), 3.68 (s, 6H, NCH_2), 2.60 (m, 12H, NCH_2 and CH_2Pyrid), 1.84 (t, 6H, J = 6.90 Hz, CH_2); ^{13}C NMR ($CDCl_3$) δ ppm: 159.20 (C-4_{phenyl}), 152.58 (C-4_{pyrid}), 151.16 (C-2_{pyrid} and C-6_{pyrid}), 139.32 (Cq_{benz}), 134.24 (C-1_{phenyl}), 130.72 (CH_{benz}), 127.28 (C-3_{phen} and C-5_{phen}), 125.27 (C-3_{pyrid} and C-5_{pyrid}), 116.22 (C-2_{phen} and C-6_{phen}), 71.11 (OCH_2), 54.69 (NCH_2), 49.81 (NCH_2), 34.22 (CH_2), 31.88 (CH_2). ESI-MS m/z $[M+H]^+$ calculated for $C_{54}H_{61}N_6$: 841.47, found: 841.4809.

3.2. Biological Evaluation

3.2.1. In Vitro Antiplasmodial Activity

Derivatives **1** were dissolved in DMSO and then diluted in sterile water in order to obtain a range of concentration from 40 nM to 40 mM for the first screening against culture-adapted *Plasmodium falciparum* reference strains 3D7 and W2. The former strain is susceptible to CQ but displays a decreased susceptibility to MQ; the latter is considered resistant to CQ. These two strains were obtained from the collection of the National Museum of Natural History (Paris, France). The parasites were cultivated in RPMI medium (Sigma-Aldrich, Lyon, France) supplemented with 0.5% Albumax I (Life Technologies Corporation, Paisley, UK), hypoxanthine (Sigma-Aldrich), and gentamicin (Sigma-Aldrich) with human erythrocytes and were incubated at 37 °C in a candle jar, as described previously [38]. The *P. falciparum* drug susceptibility test was carried out in 96-well flat-bottomed sterile plates in a final volume of 250 µL. After a 48 h incubation period with the drugs, quantities of DNA in treated and control cultures of parasites in human erythrocytes were quantified using the SYBR Green I (Sigma-Aldrich) fluorescence-based method [39,40]. Briefly, after incubation, the plates were frozen at −20 °C until use. The plates were then thawed for 2 h at room temperature, and 100 µL of each homogenized culture was transferred to a well of a 96-well flat-bottomed sterile black plate (Sigma-Aldrich, Lyon, France) that contained 100 µL of the SYBR Green I lysis buffer (2xSYBR Green, 20 mM Tris base pH 7.5, 5 mM EDTA, 0.008% *w*/*v* saponin, 0.08% *w*/*v* Triton X-100). Negative controls treated with solvent (typically DMSO or H_2O) and positive controls (CQ and MQ) were added to each set of experiments. Plates were incubated for 1 h at room temperature and then read on a fluorescence plate reader (Tecan Trading AG, Switzerland) using excitation and emission wavelengths of 485 and 535 nm, respectively. The concentrations at which the screening drug or antimalarial can inhibit 50% of parasitic growth (IC_{50}) were calculated from a sigmoid inhibition model Emax with an estimate of IC_{50} by non-linear regression (IC Estimator version 1.2) and were reported as means calculated from three independent experiments [41].

3.2.2. Cytotoxicity Evaluation

A cytotoxicity evaluation was performed using the method reported by Mosmann [42] with slight modifications to determine the CC_{50} and using doxorubicin as a cytotoxic reference compound. These assays were performed in human HepG2 cells (HB-8065) purchased from ATCC (Manassas, VA, USA). These cells are a commonly used human-hepatocarcinoma-derived cell line that has characteristics like those of primary hepatocytes. These cells express many hepatocyte-specific metabolic enzymes, thus enabling the cytotoxicity of tested product metabolites to be evaluated. Briefly, cells in 100 µL of complete RPMI medium (RPMI supplemented with 10% FCS, 1% L-glutamine (200 mM), penicillin (100 U/mL), and streptomycin (100 µg/mL)) were inoculated at 37 °C into each well of 96-well plates in a humidified chamber in 6% CO_2. After 24 h, 100 µL of medium with the test compound at various concentrations dissolved in DMSO (final concentration less than 0.5% *v*/*v*) were added, and the plates were incubated for 72 h at 37 °C. Duplicate assays were performed for each sample. Each well was microscopically examined for precipitate formation before the medium was aspirated from the wells. After aspiration, 100 µL of MTT solution (0.5 mg/mL in medium without FCS) was then added to each well. Cells were incubated for 2 h at 37 °C. The MTT solution was removed and DMSO (100 µL) was added to dissolve the resulting blue formazan crystals. Plates were shaken vigorously (300 rpm) for 5 min. The absorbance was measured at 570 nm with 630 nm as the reference wavelength in a BIO-TEK ELx808 Absorbance Microplate Reader. DMSO was used as blank and doxorubicin (Sigma Aldrich, St. Louis, MO, USA) as the positive control. Cell viability was calculated as percentage of control (cells incubated without compound). The CC_{50} was determined from the dose–response curve using TableCurve 2D V5.0 software (Systat Software, Palo Alto, CA, USA).

3.3. FRET Melting Experiments

Compounds **1** were tested for the subsequent FRET melting experiments. These were performed with dual-labeled oligonucleotides mimicking the *Plasmodium* telomeric sequences FPf1T (FAM-5′(GGGTTTA)3-GGG3′-TAMRA) and FPf8T [FAM-5′(GGGTTCA)3GGG3′-TAMRA], the human telomeric sequence F21T (FAM-(GGGTTA)3-GGG3′-TAMRA), and the human hairpin duplex sequence FdxT (FAM5′-TATAGCTATA-hexaethyleneglycol-TATAGCTATA3′-TAMRA) [16,19,43]. The oligonucleotides were pre-folded in 10 mM lithium cacodylate buffer (pH 7.2) with 10 mM KCl and 90 mM LiCl (K+ condition). The FAM emissions were recorded at 516 nm using a 492 nm excitation wavelength in the absence and presence of a single compound as a function of temperature (25 to 95 °C) in 96-well microplates by using a Stratagene MX3000P real-time PCR device at a rate of 1 °C·min^{-1}. Data were normalized between 0 and 1, and the required temperature for half denaturation of oligonucleotides corresponding to an emission value of 0.5 was taken as the Tm. Each experiment was performed in duplicate with 0.2 μM of labelled oligonucleotide and 2 μM of compound under K^+ condition. For each compound, three independent experiments were carried out.

4. Conclusions

In this research program report, we described the preparation, the antimalarial potentialities, and the in vitro cytotoxicity toward human cells of a novel series of 1,3,5-*tris*[(4-(substituted-aminomethyl)phenoxy)methyl]benzene compounds **1**. These new nitrogen polyphenoxymethylbenzene compounds were tested for their in vitro antiprotozoal activity toward the CQ-resistant W2 and CQ-sensitive 3D7 *P. falciparum* strains. Moreover, the in vitro cytotoxicity of these novel original polyaromatic derivatives was assessed on the human HepG2 cell line. Some of these newly synthesized nitrogen aromatic molecules have shown promising in vitro antiplasmodial activities with IC_{50} values in the sub and μM range against the W2 and 3D7 strains of *P. falciparum*.

In conclusion, 1,3,5-*tris*[(4-(substituted-aminomethyl)phenoxy)methyl]benzene compounds **1m** and **1p** were found as the most promising bioactive derivatives against the W2 strain, and also against the *Plasmodium* 3D7 strain. Moreover, we can also notice that this new synthesized derivative **1m** was found to be the most active compound against the CQ-resistant and MQ-sensitive *P. falciparum* strain W2 and also against the CQ-sensitive and MQ decreased sensitivity strain 3D7.

It has been previously described that the telomeres of the various parasites could constitute interesting and potential targets; thus, we also investigated the possibility of targeting *Plasmodium* telomeres by stabilizing the *Plasmodium* G-quadruplex sequences using FRET melting assays with these novel synthesized derivatives. However with regard to the stabilization of the protozoal G-quadruplex, it could be observed that the best 1,3,5-*tris*[(4-(substituted-aminomethyl)phenoxy)methyl]benzenes **1**, which exhibited an interesting stabilization profile, were not found as the most antimalarial derivatives against the two *Plasmodium* strains. Thus, no correlations between their antimalarial activities and selectivities of their respective binding to G-quadruplexes were noticed. These 1,3,5-*tris*[(4-(substituted-aminomethyl)phenoxy)methyl]benzene derivatives are unlikely to exhibit specific antimalarial activity through G-quadruplex binding mechanisms.

Furthermore, it would be intriguing to expand the pharmacological assessment of our new derivatives **1** by exploring their potential mode of action through additional studies, such as investigating the inhibition of beta-hematin formation, apicoplast functions, or resistance generation. In conclusion, these novel polyaromatic 1,3,5-*tris*[(4-(substituted-aminomethyl)phenoxy)methyl]benzenes could open the way to the design of new potential valuable and original medicinal chemistry scaffolding in antimalarial therapies.

Supplementary Materials: The following supporting information can be downloaded at: https://www.mdpi.com/article/10.3390/ddc3030035/s1. Supplementary data (Figures S1–S18) related to this article (^{1}H NMR, ^{13}C NMR, and ESI-MS of derivatives **4a–r**) are available online.

Author Contributions: J.G., S.A.-R., S.M. (Stéphane Moreau), P.S., A.C. and J.-L.M. performed the synthesis and prepared and revised the manuscript; S.A.-R., J.G. and S.S. carried out the experiments; S.A.-R., N.P., I.K., L.R. and M.M. helped in the analysis of the compounds; A.C., S.M. (Serge Moukha), P.D., P.A., C.D., R.M. and P.S. conducted the in vitro tests. All authors have read and agreed to the published version of the manuscript.

Funding: This research was funded in part by a generous grant from alumni from Ecole Polytechnique, Palaiseau, France. We also thank our respective organizations for their financial support.

Institutional Review Board Statement: Not applicable.

Informed Consent Statement: Not applicable.

Data Availability Statement: The original contributions presented in the study are included in the article/Supplementary Materials, further inquiries can be directed to the corresponding authors.

Acknowledgments: The authors would like to thank Philippe Grellier, department RDDM at Muséum National d'Histoire Naturelle (Paris, France), for generously providing the 3D7 and W2 *P. falciparum* strains.

Conflicts of Interest: The authors report no conflicts of interest. The authors alone are responsible for the content and writing of the paper.

References

1. World Health Organization. *World Malaria Report 2023*; World Health Organization: Geneva, Switzerland, 2023; Licence: CC BY-NC-SA 3.0 IGO. Available online: https://www.who.int/teams/global-malaria-programme/reports/world-malaria-report-2023 (accessed on 9 July 2024).
2. WHO Malaria. 4 December 2023. Available online: https://www.who.int/news-room/fact-sheets/detail/malaria (accessed on 9 July 2024).
3. World Health Organization. *WHO Guidelines for Malaria, 16 October 2023*; World Health Organization: Geneva, Switzerland, 2023; (WHO/UCN/GMP/ 2023.01 Rev.1). License: CC BY-NC-SA 3.0 IGO. Available online: https://app.magicapp.org/#/guideline/LwRMXj (accessed on 9 July 2024).
4. WHO Initiative to Stop the Spread of *Anopheles stephensi* in Africa, 2023 Update. Licence; CC BY-NC-SA 3.0 IGO. Available online: https://www.who.int/publications/i/item/WHO-UCN-GMP-2022.06 (accessed on 9 July 2024).
5. WHO Vector-Borne Diseases. 2020. Available online: https://www.who.int/news-room/fact-sheets/detail/vector-borne-diseases (accessed on 9 July 2024).
6. Tisnerat, C.; Dassonville-Klimpt, A.; Gosselet, F.; Sonnet, P. Antimalaria Drug Discovery: From Quinine to the Most Recent Promising Clinical Drug Candidates. *Curr. Med. Chem.* **2022**, *29*, 3326–3365. [CrossRef] [PubMed]
7. WHO Ending the Neglect to Attain the Sustainable Development Goals: A Rationale for Continued Investment in Tackling Neglected Tropical Diseases 2021–2030. Available online: https://www.who.int/publications/i/item/9789240052932 (accessed on 3 May 2023).
8. Dola, V.R.; Soni, A.; Agarwal, P.; Ahmad, H.; Raju, K.S.R.; Rashid, M.; Wahajuddin, M.; Srivastava, K.; Haq, W.; Dwivedi, A.K.; et al. Synthesis and Evaluation of Chirally Defined Side Chain Variants of 7-Chloro-4-Aminoquinoline to Overcome Drug Resistance in Malaria Chemotherapy. *Antimicrob. Agents Chemother.* **2017**, *61*, e01152-16. [CrossRef] [PubMed]
9. Rathod, G.K.; Jain, M.; Sharma, K.K.; Das, S.; Basak, A. New structural classes of antimalarials. *Eur. J. Med. Chem.* **2022**, *242*, 114653. [CrossRef]
10. Dhameliya, T.M.; Patel, D.S.; Kathuria, D.; Shah, M.B.; Dabhabe, A.S.; Dave, H.S.; Lad, N.C.; Chaudhari, A.Z.; Alom, S.; Vyas, V.K.; et al. Biannual account of anti-malarial agents reported in 2021 and 2022: A comprehensive coverage. *ChemistrySelect* **2024**, *9*, e202303982. [CrossRef]
11. Abd-Rahman, A.; Zaloumis, S.; McCarthy, J.; Simpson, J.; Commons, R. Scoping Review of Antimalarial Drug Candidates in Phase I and II Drug Development. *Antimicrob. Agent. Chemother.* **2022**, *26*, e01659-21. [CrossRef]
12. Perko, N.; Kebede, T.; Mousa, S. Current and future directions in the prevention and treatment of Malaria. *J. Pharm. Pharmacol. Res.* **2022**, *6*, 131–138. [CrossRef]
13. Van de Walle, T.; Cools, L.; Mangelinckx, S.; D'hooghe, M. Recent contributions of quinolines to antimalarial and anticancer drug discovery research. *Eur. J. Med. Chem.* **2021**, *226*, 113865. [CrossRef]
14. Goyal, A.; Kharkwal, H.; Piplani, M.; Singh, Y.; Murugesan, S.; Aggarwal, A.; Kumar, P.; Chander, S. Spotlight on 4-substituted quinolines as potential anti-infective agents: Journey beyond chloroquine. *Arch. Pharm.* **2023**, *356*, e2200361. [CrossRef]
15. Guillon, J.; Grellier, P.; Labaied, M.; Sonnet, P.; Léger, J.-M.; Déprez-Poulain, R.; Forfar-Bares, I.; Dallemagne, P.; Lemaître, N.; Péhourcq, F.; et al. Synthesis, antimalarial activity, and molecular modeling of new pyrrolo[1,2-*a*]quinoxalines, bispyrrolo[1,2-*a*]quinoxalines, bispyrido[3,2-*e*]pyrrolo[1,2-*a*]pyrazines, and bispyrrolo[1,2-a]thieno[3,2-*e*]pyrazines. *J. Med. Chem.* **2004**, *47*, 1997–2009. [CrossRef]

16. Dassonville-Klimpt, A.; Cézard, C.; Mullié, C.; Agnamey, P.; Jonet, A.; Da Nascimento, S.; Marchivie, M.; Guillon, J.; Sonnet, P. Absolute Configuration and Antimalarial Activity of erythro-Mefloquine Enantiomers. *ChemPlusChem* **2013**, *78*, 642–646. [CrossRef]
17. Guillon, J.; Cohen, A.; Gueddouda, N.M.; Das, R.N.; Moreau, S.; Ronga, L.; Savrimoutou, S.; Basmaciyan, L.; Monnier, A.; Monget, M.; et al. Design, synthesis and antimalarial activity of novel bis{*N*-[(pyrrolo[1,2-*a*]quinoxalin-4-yl)benzyl]-3-aminopropyl}amine derivatives. *J. Enzym. Inhib. Med. Chem.* **2017**, *32*, 547–563. [CrossRef] [PubMed]
18. Jonet, A.; Guillon, J.; Mullie, C.; Cohen, A.; Bentzinger, G.; Schneider, J.; Taudon, N.; Hutter, S.; Azas, N.; Moreau, S.; et al. Synthesis and Antimalarial Activity of New Enantiopure Aminoalcoholpyrrolo[1,2-*a*]quinoxalines. *Med. Chem.* **2018**, *14*, 293–303. [CrossRef]
19. Dassonville-Klimpt, A.; Schneider, J.; Damiani, C.; Tisnerat, C.; Cohen, A.; Azas, N.; Marchivie, M.; Guillon, J.; Mullié, C.; Agnamey, P.; et al. Design, synthesis, and characterization of novel aminoalcohol quinolines with strong in vitro antimalarial activity. *Eur. J. Med. Chem.* **2022**, *228*, 113981. [CrossRef] [PubMed]
20. Guillon, J.; Cohen, A.; Nath Das, R.; Boudot, C.; Meriem Gueddouda, N.; Moreau, S.; Ronga, L.; Savrimoutou, S.; Basmaciyan, L.; Tisnerat, C.; et al. Design, synthesis, and antiprotozoal evaluation of new 2,9-bis[(substituted-aminomethyl)phenyl]-1,10-phenanthroline derivatives. *Chem. Biol. Drug Des.* **2018**, *91*, 974–995. [CrossRef] [PubMed]
21. Guillon, J.; Cohen, A.; Monic, S.; Boudot, C.; Savrimoutou, S.; Albenque-Rubio, S.; Moreau, S.; Dassonville-Klimpt, A.; Mergny, J.-L.; Ronga, L.; et al. Synthesis and antiprotozoal evaluation of new 2,9-bis[(pyridinylalkylaminomethyl)phenyl]-1,10-phenanthroline derivatives by targeting G-quadruplex, an interesting pharmacophore against drug efflux. *Acta Sci. Pharm. Sci.* **2023**, *7*, 50–65. [CrossRef]
22. Guillon, J.; Cohen, A.; Boudot, C.; Monic, S.; Savrimoutou, S.; Moreau, S.; Albenque-Rubio, S.; Lafon-Schmaltz, C.; Dassonville-Klimpt, A.; Mergny, J.-L.; et al. Design, synthesis, biophysical and antiprotozoal evaluation of new promising 2,9-bis[(substituted-aminomethyl)]-4,7-phenyl-1,10-phenanthroline derivatives by targeting G-quadruplex, a potential alternative to drug efflux. *Pathogens* **2022**, *11*, 1339. [CrossRef]
23. Albenque-Rubio, S.; Guillon, J.; Cohen, A.; Agnamey, P.; Savrimoutou, S.; Moreau, S.; Mergny, J.-L.; Ronga, L.; Kanavos, I.; Moukha, S.; et al. Synthesis and Antimalarial Evaluation of New 1,3,5-*tris*[(4-(Substitutedaminomethyl)phenyl)methyl]benzene Derivatives: A Novel Alternative Antiparasitic Scaffold. *Drugs Drug Candidates* **2023**, *2*, 653–672. [CrossRef]
24. Antonijevic, M.; Rochais, C.; Dallemagne, P. C3-Symmetric Ligands in Drug Design: When the Target Controls the Aesthetics of the Drug. *Molecules* **2023**, *28*, 679. [CrossRef]
25. Calvo, E.P.; Wasserman, M. G-Quadruplex ligands: Potent inhibitors of telomerase activity and cell proliferation in *Plasmodium falciparum*. *Mol. Biochem. Parasitol.* **2016**, *207*, 33–38. [CrossRef]
26. Tidwell, R.R.; Boykin, D.W.; Ismail, M.A.; Wilson, W.D.; White, E.W.; Kumar, A.; Nanjunda, R. Dicationic compounds which selectively recognize G-quadruplex DNA. US Patent EP 1792613A2, 6 June 2007.
27. Leeder, W.-M.; Hummel, N.F.C.; Göringer, H.U. Multiple G-quartet structures in pre-edited mRNAs suggest evolutionary driving force for RNA editing in trypanosomes. *Sci. Rep.* **2016**, *6*, 29810. [CrossRef]
28. Lombrana, R.; Alvarez, A.; Fernandez-Justel, J.M.; Almeida, R.; Poza-Carrion, C.; Gomes, F.; Calzada, A.; Requena, J.M.; Gomez, M. Transcriptionally Driven DNA Replication Program of the Human Parasite *Leishmania major*. *Cell Rep.* **2016**, *16*, 1774–1786. [CrossRef] [PubMed]
29. Bottius, E.; Bakhsis, N.; Scherf, A. *Plasmodium falciparum* Telomerase: De Novo Telomere Addition to Telomeric and Nontelomeric Sequences and Role in Chromosome Healing. *Mol. Cell. Biol.* **1998**, *18*, 919–925. [CrossRef] [PubMed]
30. Wakai, T.N.; Anzaku, D.O.; Afolabi, I.S. Telomeres and telomerase as promising targets for malaria therapy: A comprehensive review. *Preprints* **2024**, 2024041000. [CrossRef]
31. Raj, D.K.; Das, D.R.; Dash, A.P.; Supakar, P.C. Identification of telomerase activity in gametocytes of *Plasmodium falciparum*. *Biochem. Biophys. Res. Commun.* **2003**, *309*, 685–688. [CrossRef]
32. De Cian, A.; Grellier, P.; Mouray, E.; Depoix, D.; Bertrand, H.; Monchaud, D.; Telade-Fichou, M.-P.; Mergny, J.-L.; Alberti, P. *Plasmodium* Telomeric Sequences: Structure, Stability and Quadruplex Targeting by Small Compounds. *ChemBioChem* **2008**, *9*, 2730–2739. [CrossRef]
33. Rajakumar, P.; Swaroop, M.; Jayavelu, S.; Murugesan, K. Synthesis, complexation studies and biological applications of some novel stilbenophanes, indolophanes and bisindolostilbenophanes via McMurry coupling. *Tetrahedron* **2006**, *62*, 12041–12060. [CrossRef]
34. Diab, H.; Abdelhamid, I.; Elwahy, A. ZnO-Nanoparticles-Catalysed Synthesis of Poly(tetrahydrobenzimidazo[2,1-*b*]quinazolin-1(2*H*)-ones) as Novel Multi-armed Molecules. *Synlett* **2018**, *29*, 1627–1633.
35. Full Crystallographic Results Were Deposited at the Cambridge Crystallographic Data Centre (CCDC-2358055). Supplementary X-ray Crystallographic Data: Cambridge Crystallographic Data Centre, University Chemical Lab, Lensfield Road, Cambridge, CB2 1EW, UK. Available online: https://www.ccdc.cam.ac.uk/ (accessed on 3 June 2024).
36. Ramirez, T.; Strigun, A.; Verlohner, A.; Huener, H.A.; Peter, E.; Herold, M.; Bordag, N.; Mellert, W.; Walk, T.; Spitzer, M.; et al. Prediction of liver toxicity and mode of action using metabolomics in vitro in HepG2 cells. *Arch. Toxicol.* **2018**, *92*, 893–906. [CrossRef]
37. Rodriguez-Antona, C.; Donato, M.T.; Boobis, A.; Edwards, R.J.; Watts, P.S.; Castell, J.V.; Gómez-Lechón, M.J. Cytochrome P450 expression in human hepatocytes and hepatoma cell lines: Molecular mechanisms that determine lower expression in cultured cells. *Xenobiotica* **2002**, *32*, 505–520. [CrossRef]

38. Desjardins, R.E.; Canfield, C.J.; Haynes, J.D.; Chulay, J.D. Quantitative assessment of antimalarial activity in vitro by a semiautomated microdilution technique. *Antimicrob. Agents Chemother.* **1979**, *16*, 710–718. [CrossRef]
39. Bennett, T.N.; Paguio, M.; Gligorijevic, B.; Seudieu, C.; Kosar, A.D.; Davidson, E.; Roepe, P.D. Novel, Rapid, and Inexpensive Cell-Based Quantification of Antimalarial Drug Efficacy. *Antimicrob. Agents Chemother.* **2004**, *48*, 1807–1810. [CrossRef] [PubMed]
40. Bacon, D.J.; Latour, C.; Lucas, C.; Colina, O.; Ringwald, P.; Picot, S. Comparison of a SYBR Green I-Based Assay with a Histidine-Rich Protein II Enzyme-Linked Immunosorbent Assay for In Vitro Antimalarial Drug Efficacy Testing and Application to Clinical Isolates. *Antimicrob. Agents Chemother.* **2007**, *51*, 1172–1178. [CrossRef]
41. Kaddouri, H.; Nakache, S.; Houzé, S.; Mentré, F.; Le Bras, J. Assessment of the Drug Susceptibility of *Plasmodium falciparum* Clinical Isolates from Africa by Using a *Plasmodium* Lactate Dehydrogenase Immunodetection Assay and an Inhibitory Maximum Effect Model for Precise Measurement of the 50-Percent Inhibitory Concentration. *Antimicrob. Agents Chemother.* **2006**, *50*, 3343–3349. [PubMed]
42. Mosmann, T. Rapid colorimetric assay for cellular growth and survival: Application to proliferation and cytotoxicity assays. *J. Immunol. Methods* **1983**, *65*, 55–63. [CrossRef] [PubMed]
43. De Cian, A.; Guittat, L.; Kaiser, M.; Saccà, B.; Amrane, S.; Bourdoncle, A.; Alberti, P.; Teulade-Fichou, M.-P.; Lacroix, L.; Mergny, J.-L. Fluorescence-based melting assays for studying quadruplex ligands. *Methods* **2007**, *42*, 183–195. [CrossRef]